A PROTOCOL FOR ACHIEVING ADHERENT CELL CULTURE WITHIN A MICROFLUIDIC DEVICE

A Thesis

presented to

the Faculty of California Polytechnic State University,

San Luis Obispo

In Partial Fulfillment

of the Requirements for the Degree

Master of Science in Biomedical Engineering

by

Tarra Danielle Sanders

December 2020

COMMITTEE MEMBERSHIP

TITLE: A Protocol for Achieving Adherent Cell Culture within a Microfluidic Device

AUTHOR: Tarra Danielle Sanders

DATE SUBMITTED: December 2020

COMMITTEE CHAIR: Benjamin Hawkins, Ph.D.
Professor of Biomedical Engineering

COMMITTEE MEMBER: Davide Clague, Ph.D.
Professor of Biomedical Engineering

COMMITTEE MEMBER: Christopher Heylman, Ph.D.
Assistant Professor of Biomedical Engineering

ABSTRACT

A Protocol for Achieving Adherent Cell Culture within a Microfluidic Device

Tarra Danielle Sanders

The goal of this study is to design a protocol for the adherent cell culture within a novel microfluidic device. Microscale cell culture protocols were developed for loading cells using poly-L-lysine to enhance adherent cell culture of murine derived NIH 3T3 fibroblasts. This work sought to develop a method for adherent microculture by examining various sterilization, surface treatment, and seeding techniques. Using a vacuum suction loading technique, air plasma treatment and a poly-L-lysine surface treatment adherent cell culture was observed within the device. The work presented here is part of a collaborative effort that aims to develop protocols for the electrical and optical characterization of cell culture within a novel microfluidic device.

ACKNOWLEDGMENTS

To Dr. Benjamin Hawkins: Thank you for allowing me to participate in this incredible project. Thank you for inspiring my academic passions and encouraging me every step of the way. I am forever grateful for the time I worked with you, both as a student and as a colleague.

To my committee members, Dr. David Clague and Dr. Christopher Heylman: Thank you for your mentorship and support. Thank you for your insight and expertise throughout my academic career. I am honored to have had the opportunity to work with such great scientists and engineers.

To my parents: Thank you for always believing in me, regardless of my pursuits. Thank you for your unwavering support and love, without you none of this would have been possible. You are my inspirations.

To my siblings: Thank you for your unconditional love and support. You were always there to help me, from physics to drafting to late night philosophical discussions. None of this would have been the same without you by my side. You are forever my role models and inspirations.

TABLE OF CONTENTS

LIST OF TABLES

LIST OF FIGURES

Figure Page

1. INTRODUCTION

The basic principles of *in-vitro* cell culture technique used today were developed in the early twentieth century [1]. In 1916, Rous et. al discovered the importance of trypsin for obtaining cell suspension and subsequently plating individual cells [2]. Their work showed that "individual, living, tissue cells can be obtained in suspension by digesting with trypsin the clot of growing tissue cultures" [2]. Trypsin is an enzyme that works by digesting the extracellular matrix (ECM). The ECM is a network of collagen, enzymes, and glycoproteins that not only provides structural support, but also plays a crucial role in the biomechanical and biochemical signaling of cellular networks [3]. Furthermore, they were able to show that when the cells were re-plated and washed with fresh media, the cells proliferated and reformed their cellular networks.

In 1963, Todaro and Green established the first well behaved, contact-inhibited cell line: the 3T3 cell line [4]. The fascinating part about this cell line is that it can be inoculated at a lower density, 3×10^5 cells per 20 cm^2, and passaged every three days, while the recommended seeding density for other cell lines in a 25 cm^2 flask is 7×10^5 cells [31]. Due to their contact inhibition, these cells do not grow over each other and the size of the cells remains consistent with each passage [4]. Furthermore, this is an immortal cell line, or as defined by Hayflick, a cell line "capable of indefinite survival in conditions where no changes have occurred in molecular composition from some arbitrary beginning" [5]. Due to this immortality, 3T3 is a very robust, durable cell line, making it an ideal candidate for preliminary testing of cell culture in a microfluidic device.

A goal of cell and tissue culture is to recreate the cells specific *in-vivo* environment *in-vitro*. However, it is difficult to control an environment when working with length scales that differ by orders of magnitude. The average size of a human cell is 10-100μm, whereas the average size of a petri-dish is a 100mm, and tissue culture flasks are even larger. Traditional tissue culture methods use T-75, 150, and 175 cm^2 flasks requiring media volumes of 7.5, 22.5, and 52.5 mL, respectively. At the macro-scale, traditional culture methods can use liters of solutions and media in a given week, or even a single day. In contrast, current commercially available microfluidic devices can use as little as 10 to 20 milliliters of solutions, media, and reagents a week.

With the advancements in recent technologies such as micro total analysis systems (μTAS) and lab on a chip (LOC) systems, scientists are now able to work on length scales more closely approximating those found in *in-vivo* environments. However, the well-defined processes for cell culture at the macroscale level do not linearly translate to the microscale. Different phenomena dominate at the microscale compared to macroscale.

1.1 Microfluidics

Microfluidics is the science of manipulating fluids in micro- and nano- scale geometries. Two key players in the advancement of microelectromechanical systems (MEMs) were the semiconductor industry and the military. In the 1950s, photolithography was developed as a way to manufacture electronic devices that could be used for military applications. In that same decade, Kilby and Noyce invented integrated circuits (ICs). Initial ICs were fabricated using germanium. The inherent limitations of germanium led to the use of silicon, which is still commonly used in MEMs fabrication to date [32].

From photolithography, soft lithography and replica molding using poly (dimethyl siloxane) were developed in the 1980s, paving the way for microfluidic device fabrication for biological applications [26, 32]. Compared to photolithography, soft lithography is more affordable and less time intensive, which helps save research scientists time and money.

Microfluidics enable higher specificity within a given experiment. This is especially ideal when working with biological systems and trying to recreate the *in-vivo* conditions *in-vitro*. The other well cited advantages of microfluidics are small reagents samples, reduced turnaround times, and higher throughput.

1.2 Soft Lithography

Traditional cleanroom photolithography techniques are used to fabricate a master mold of the microfluidic device. For this work, the CAD drawing of the microfluidic device used to fabricate the SU8 master mold is shown in **Figure 1.2**. Traditional soft-lithography techniques and replica molding are used to quickly manufacture multiple ready-to-use microfluidic devices.

Poly(dimethyl siloxane) (PDMS) is a polymeric material commonly used in biological systems because it is relatively bio-inert and biocompatible. PDMS is transparent with a low autofluorescence and a recorded index of refraction of 1.4 [6]. It is also permeable to most gases, importantly CO_2, and impermeable to water, helping preserve the sterility and integrity of an experiment. These properties make it ideal for applications involving microscopy and fluorescence analysis, like many cellular assays. However, PDMS is not entirely inert and is permeable to small hydrophobic materials like many drugs [7, 30], which are important considerations when designing cellular assays.

PDMS is used for soft lithography replica molding in the manufacturing of certain microfluidics. Air plasma treatment is used in the manufacturing process for the adhesive bonding of the PDMS to the desired substrate. For this work, the PDMS mold is irreversibly bonded to a glass slide, creating the final form of the device shown in **Figure 1.1** below.

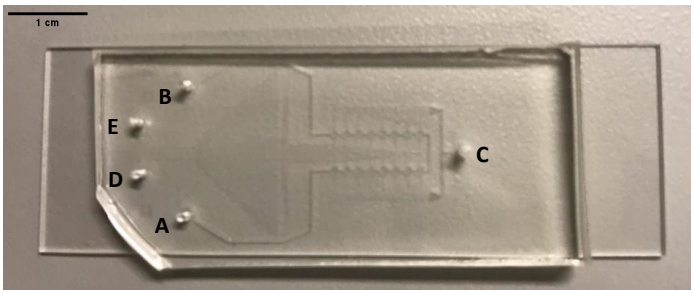

Figure 0.1 Microfluidic Device Examined in this Work: Final product developed using soft lithography replica molding. A) inlet to the cell culture network. B) outlet of cell culture network. C) outlet for the entire system. D) and E) inlets to the concentration gradient generator.

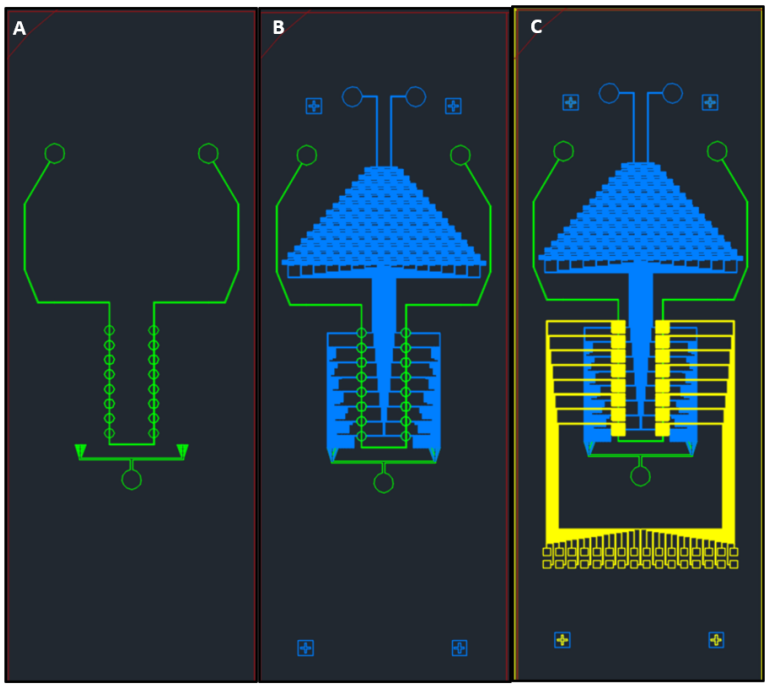

Figure 0.2 CAD Drawing of Microfluid Device: The green network is the cell culture network (A), the blue network is the concentration gradient and feeding network (B), and the yellow network is the interdigitated electrode array (C).

1.3 Gradient Generators

Biomolecular gradients play a crucial role in biological processes like inflammation, wound healing, and cancer. Biomolecular gradients also play a role in the growth, differentiation, and migrations of cells *in-vivo* [19]. The signaling protein gradients used to guide the growth, differentiation, and migration of developing cells are highly spatially and temporally regulated [19]. Using microfluidics, it is possible to create concentration gradients on a length scale that is suitable for cellular assays. Furthermore, microfluidic gradients are quantifiable, reproducible, and predictable [19].

Gradient generators also have applications for drug dosing and toxicity assays. Macroscale drug dosing requires manual creation of the required drug concentrations, which is not only time intensive, but also prone to human error.

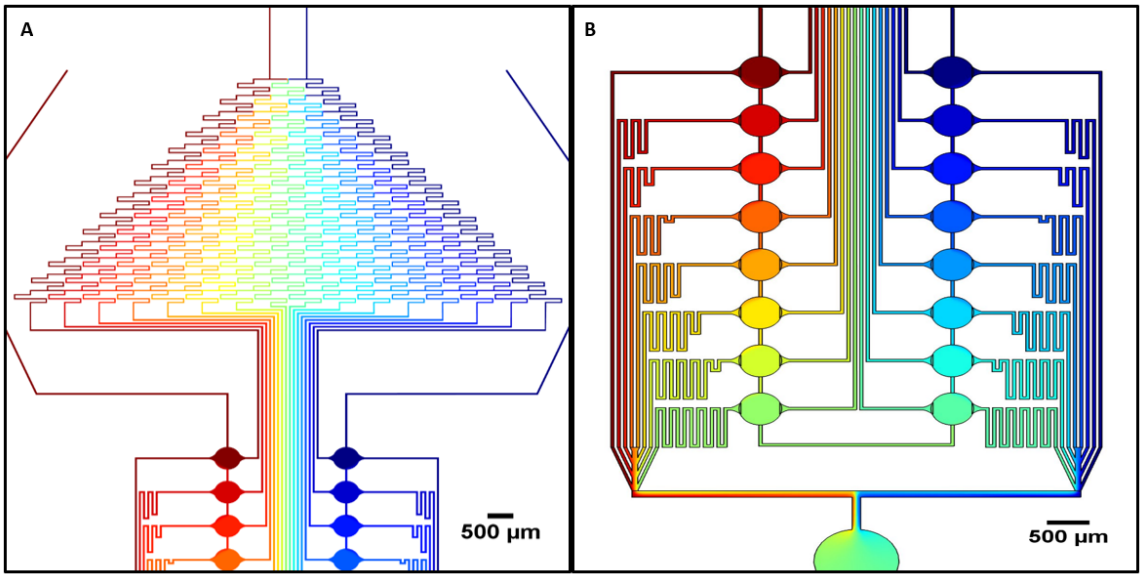

Figure 0.3 Christmas Tree Gradient Generator: COMSOL model of concentration gradient network. Red and Blue are the initial solute concentrations. [20]

The device examined in this work used the "Christmas Tree Gradient Generator" design to create 16 unique concentrations. The complex branching network is used to mix the two initial concentrations. Generating homogenous mixtures on the micro- and nano-length scales requires consideration of the rate of diffusion and the flow rate. Based on the dimensions of microfluidic devices, fluid flow within the device tends to be laminar.

1.4 Electrical Impedance Spectroscopy

Biological cells exhibit certain responses to electrical stimulation that scientists can use as a means to measure and quantify the overall health of a system. Electrical impedance spectroscopy or electrochemical impedance spectroscopy is a highly sensitive,

nondestructive characterization technique that is used to establish the chemical or electrical response of a system [9]. Impedance spectroscopy can be used in cellular assays to provide information regarding the cell population, cell proliferation, and cell death. It can also provide useful information on the fluid properties, like ionic concentrations within the media.

Electrical impedance is a measure of the system's ability to resist flow from an applied voltage at varying frequencies. The impedance, or complex electrical resistance, of the system is related to its ability to resist the flow of electrical current [10]. The impedance of a system is a complex number calculated using the resistance, inductance, and capacitive elements, as shown in the equations below:

$$Z = R + jX \tag{2.1}$$

$$Z = \frac{I}{V} \tag{2.2}$$

Where Z is the complex impedance, R is the real resistance, and X is the reactance. The real resistance, shown in **equation 2.2,** is calculated using Ohm's law and is a ratio of the current to applied voltage. The reactance is the sum of the inductive and capacitive reactance of the system. As a measure of the system's response to change in frequencies, reactance is a complex number denoted by "j." Unlike reactance, the resistance of the system is not affected by the frequency.

In cells, the phospholipid bilayer membrane acts like an electric capacitor by storing and impeding the current flow [27]. The impedance properties of cells can be used to characterize *in-vitro* cell culture. In i*n-vitro* environments most cells are anchorage

dependent [13]. Meaning that cells need to attach to a substrate in order to survive and proliferate. Using photolithography techniques, it is possible to pattern an electrode array on a substrate that can be used for adherent cell culture. As shown in **Figure 1.2C** the device presented here includes an interdigitated electrode array that is patterned onto a glass substrate. Prior to cells being introduced to the device the impedance of the system will be relatively low, electrolytes and ions in the media will result in a baseline impedance. After cells are introduced the impedance of the system will slowly increase as the cells settle and attach to the electrodes surface. The overall impedance of the system will increase as the confluency increases. The more cells present within the device the greater the impedance of the system to electrical current. Likewise, if the cells begin to die and detach, or experience various morphological changes that decrease the confluency, the impedance of the system will decrease. Electrical measurements provide quantifiable information on *in-vitro* cell culture that can be used to characterize the overall health of the system. Providing a higher level of information than traditional microscopy techniques alone.

1.4.1 Electric Double Layer

The electric double layer describes a phenomenon occurring at the interface of an electrode (or substrate) in an electrolytic solution. Most substances will acquire a surface electric charge when submerged in an aqueous solution [11]. To balance out the surface electric charge, counterions are attracted to the surface while coions are repelled. The electric double layer is the result of these ionic attractions and repulsions. At the surface, there is a higher number of counterions than coions, resulting in a non-neutral surface charge, highlighted in the figure below.

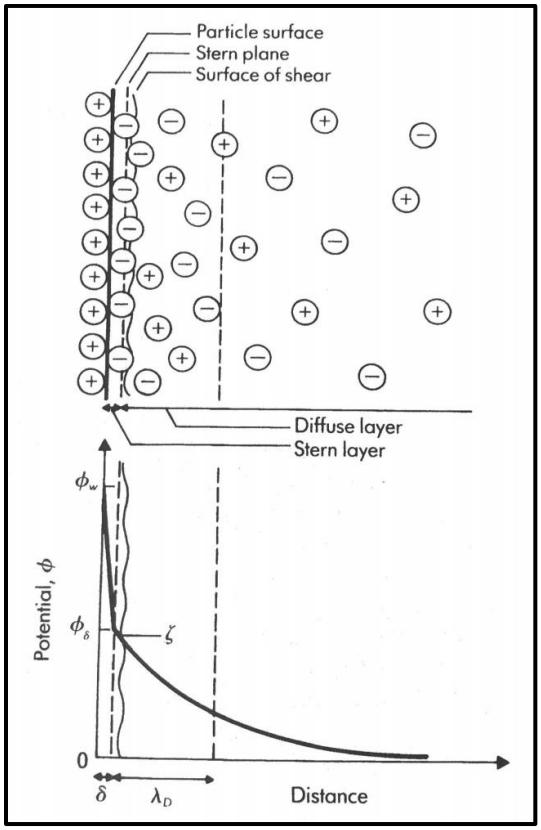

Figure 0.4 The Electric Double Layer: The structure of the electric double layer. [11]

In microfluidic systems, the effects of the electric double layer are dominant and reduce the sensitivity to the intrinsic impedance of the fluid (and substrate) below a characteristic frequency [12]. The impact of the double layer in this system is an important consideration and impedance measurements of the system should be calibrated to account for the effects of the electric double layer.

1.5 Cell Culture

Most mammalian cells *in-vitro* are anchorage dependent [13]. The anchorage of the cell to the substrate is paramount to its ability to grow and proliferate in *in-vitro* environments. Most commercially available tissue culture flasks and well plates are

manufactured using polystyrene [28]. The polystyrene culture surface is plasma treated, which activates the surface and promotes the adhesion of various cells. Plasma treatments also sterilize the device, reducing the risk of contamination.

Many factors play a role when recreating the cellular microenvironment. A growth substrate can be used to enhance the surface for cell adhesion, growth, and proliferation[14]. The surface can be coated with proteins like laminin and collagen, or polymers like Poly-L-Lysine (PLL) and Poly-D-Lysine [30]. The specific growth substrate usually depends on cell type and experimental design. Cells can secrete different factors whether they are in suspension or adhered, and if they are 'stressed' [24]. It is important to keep these considerations in mind when running experimental assays because cells can behave differently in different microenvironments, which could impact the efficacy of the work.

Another important component utilized to recreate the appropriate microenvironment is the media and components added to the media that are used to feed and supply nutrients to the cells. The media consists of two basic components: a basal nutrient medium and supplements [14]. Amino acids and vitamins, ions, serums, and other components can be added to the media. In this work, our media solution contains a basal medium, fetal bovine serum, antibiotics, and antifungal solutions.

Lastly, it is importantly to strictly regulate the physio-chemical properties of the cultures *in-vitro*. Potential Hydrogen (pH) is an important component of the cellular microenvironment. In many medias, Phenol Red is used as a visual pH indicator. Most mammalian cells have a pH between 7.0-7.4. Cells stop growing between 7.0-6.5 and viability is lost below 6.5. [14]. It is worth noting that some cells, such as fibroblasts,

require a higher pH for optimal conditions. Fibroblasts' niche can have a pH between 7.4-7.7. It is also important to regulate the supplies of CO_2 and oxygen *in-vitro.* Most scientific incubators are kept at physiological temperature, 37°C, with ~5% CO_2 and a relative humidity of 95%, however CO_2 concentrations and relative humidity can vary depending on cell and culture type. CO_2 is dissolved into culture mediums to help establish proper physiological pH conditions for cell culture [14]. As cells metabolize and proliferate, they produce more CO_2 decreasing the overall pH of the system. Sodium bicarbonate is added to culture mediums as a buffering agent to help regulate the fluctuations of the pH in the presence of CO_2 [14].

1.6 Cell Response

Cells respond to stress in a variety of ways from activation of pathways that promote survival to inducing programmed cell death [34]. Stress impinges upon the systems physiological ability to maintain homeostasis. A physiological system can withstand a certain level of stress by signaling for an appropriate protective cellular response [34]. However, if the stress to the system is too extreme or prolonged for a sufficient amount of time cellular signaling cascades results in apoptosis, necrosis, pyroptosis, or autophagic cell death [34]. The ability to measure and quantify these responses is a large component of drug and toxicity assays *in-vitro.* The combination of electrical and optical measurement methods presented in this work can be used to provide a finer level of detail and quantify the cellular response to specific stressors.

1.7 Microculture

In part due to the availability of information for traditional cell culture, some of these conditions are easier to regulate at the macroscale. Microfluidic cell culture, however, is still relatively novel, so many of these conditions are still being developed and fine-tuned.

In microculture, the surface-area-to-volume ratio is much greater than traditional macro-culture techniques. In other words, if the same cell culture density is used in a microchannel and a well culture plate, the volume per cell is significantly reduced in the microculture system [15]. This can be both advantageous and disadvantageous. On one hand, it can enable the development of *in-vitro* models for paracrine signaling that had previously been difficult using traditional culture techniques [13]. However, it also poses challenges for microculture due to the quick depletion of nutrients and rapid accumulation of waste in the culture media within a device. These limitations are important to consider when developing a microfluidic system for cell culture.

2. BACKGROUND

2.1 Effective Culture Time

The maintenance of cell culture relies on regular media changes at precise time intervals. The dimensionless parameter Da, or Damköhler number, is a measure of the reaction velocity with respect to the diffusion velocity [11]. The Damköhler number can be used to help determine the optimal interval for replacing media within the microfluidic device.

$$D_a = \frac{K_m h \sigma}{D C_0} \tag{2.3}$$

Where K_m is the substrate uptake rate by the cells, D is the diffusivity of the substrate, C_0 is the initial concentration of the particular substrate, σ is the cell density, and h is the height of the channel.

Or, written another way:

$$D_a = \frac{\frac{h^2}{D}}{\frac{C_0 h}{K_m \sigma}} \tag{2.4}$$

Where the numerator represents the diffusion time scale, h^2/D, and the denominator represents the reaction time scale, $C_0 h/K_m \sigma$. The reaction time dictates the speed of the process because diffusion to the top of the microchannel happens much more quickly than the reaction of all the substrate at the bottom [16]. The Effective Culture Time (ECT) is the time interval between media changes in a microfluidic system. A key

obstacle to overcome in microculture is accounting for the high surface-area-to-volume ratios in microfluidic systems and replenishing the nutrients within the system sufficiently based on these constraints. In a diffusion dominant system, the reaction time is equivalent to the effective culture time, which is proportional to the height of the channel. Therefore, the ECT can be approximated based on the height of the microchannel.

Based on literature, a $200\ \mu m$ deep channel requires media perfusion every 8-12 hours to maintain ideal culture conditions [17]. Assuming an approximately linear relationship, $ECT \propto$ h , a device with a channel depth of $70\ \mu m$ requires fresh media every 2.8-4.2 hours.

2.2 Critical Perfusion Rate

The critical perfusion rate (CPR) can help determine the volumetric flow rate necessary to properly replenish nutrients and media within the device. Another dimensionless parameter, κ, can be derived for the ratio of convection and reaction time scales [16], shown in **Equation 2.5** below:

$$\kappa = \frac{\frac{L}{U_m}}{\frac{C_0 h}{K_m \sigma}} = \frac{L K_m \sigma}{U_m C_0 h} \tag{2.5}$$

Where h represents the height of the channel, L is the length of the channel, U_m is the constant flow velocity, K_m is the substrate uptake rate by the cells, C_0 is the initial concentration of the particular substrate, and σ is the cell density.

Sufficient perfusion, wherein the media and nutrients travel the entire length of the device before being depleted in the device, requires $\kappa \geq 1$. Knowing that the effective culture time is equivalent to the reaction time **equation 2.4** can be simplified, as shown below in **equation 2.6.**

$$CPR = U_m(\kappa = 1) = \frac{LK_m\sigma}{C_0 h} = \frac{L}{\tau_r} \tag{2.6}$$

Where τ_r denotes the reaction time scale and is equivalent to the height of the channel squared divided by the diffusivity of the substrate. A $\kappa = 1$ is assumed to establish the minimum flow rate required to properly perfuse the system.

Therefore, the critical perfusion rate of a device is the length of the channel divided by the effective culture time. The length of the cell network presented in this device is ~500μm and ~70μm deep. Based on literature, and **equation 2.6** presented above, the ideal perfusion rate for this device would be between 105 $\frac{\mu m}{hr}$ and 220 $\frac{\mu m}{hr}$ [14]. To determine an ideal volumetric flow rate, equation 2.7 below is used.

$$Q = A \times \vec{v} \tag{2.7}$$

Where Q is the volumetric flow rate, A is the cross sectional area, and $\vec{v}$ is the average velocity of the fluid.

Using equation 2.7, and assuming an approximate cross-sectional area of the device as 4×10^5 μm^2, a minimum perfusion rate between $0.05\frac{\mu L}{hr}$ and $0.1\frac{\mu L}{hr}$ is required to replenish nutrients in the system. Through the cell network a higher flow rate may still be

required for sufficient perfusion as the overall confluency of the system increases. However, the goal of the device is to use the gradient generator, which delivers fresh media to every well, without any concern of the nutrients being depleted before reaching any specific well.

2.3 Rhodamine 123

Various assays exist for the labeling and optical analysis of cell cultures. Some techniques use antibody labeling and immunofluorescence to detect the presence of specific biomarkers, proteins, or cell types. There are live/dead stains and nuclear stains, like Trypan Blue and DAPI. Finally, there are metabolic stains, like Rhodamine. Using fluorescent microscopy, the expression and level of expression of specific markers can be analyzed and quantified to provide information about the cellular system.

In widefield fluorescence microscopy a parallel beam of light is used to excite fluorophores within a sample of interested [35].Traditionally, a mercury or xenon high pressure bulb is used to provide the excitation light [35]. A mercury arc lamp source was filtered using a standard FITC fluorescence filter cube to isolate excitation and emission spectra for fluorescence images in this work. With this filter, excitation was provided by blue light, 400-525 nm. The fluorophore in Rhodamine 123 absorbs blue light, 505 nm, and emits green light, 534 nm [22]. Extra care was taken to preserve the samples and prevent photo-bleaching.

At the macroscale, this work used Rhodamine 123 (Rh123) to examine the metabolic activity of fibroblasts cultured in media containing varying amounts of glucose. Rhodamine 123 is a cationic fluorescent dye that labels the mitochondria. The lipophilic nature of Rh123 allows it to diffuse across the mitochondrial membrane in response to

potential and concentration gradients [18]. A loss in potential results in less accumulation of dye in the membrane and decreased fluorescence intensity that could be used as a method to characterize cell health. **Figure 2.1** below shows two samples with varying expression rates of Rh 123, Images B and E were obtained using a widefield fluorescent microscope and FITC filter as describe above.

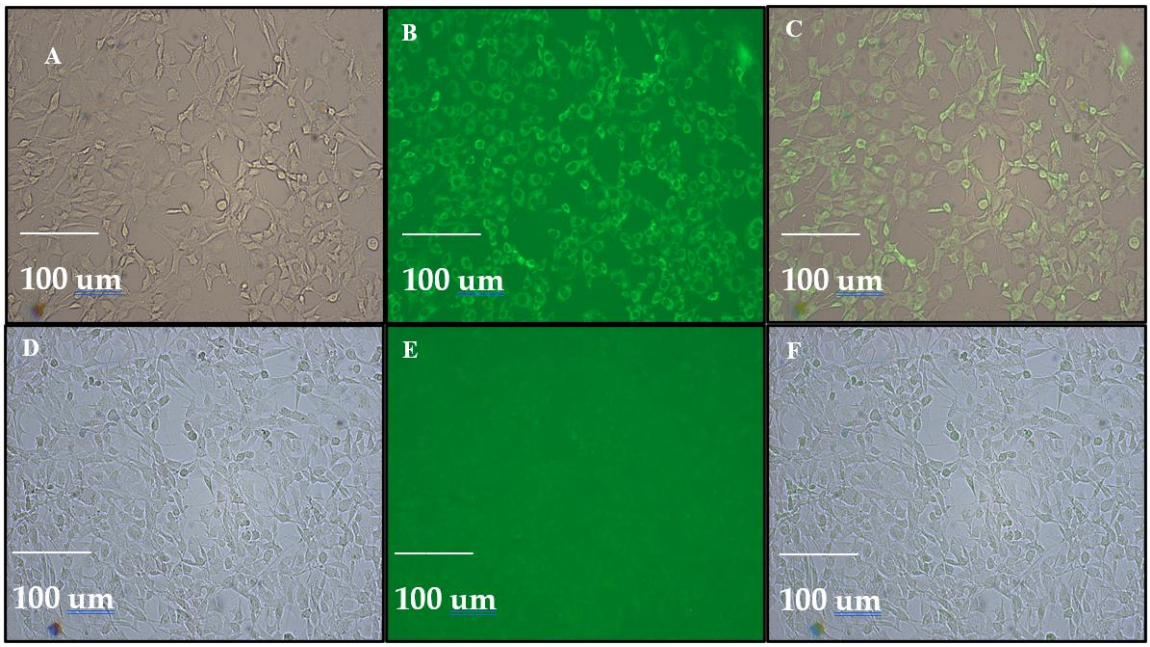

Figure 0.1 Wide-Field Fluorescence Microscopy Images of Fibroblasts stained with RH 123. The images presented above show varying rates of Rhodamine 123 expression in murine derived NIH 3T3 fibroblasts cultured in a tissue treated 6-well plate. Images A and D are brightfield images, Image B and E are fluorescent images using a FITC filter, and C and F are stacked brightfield-fluorescent images obtained using NIH ImageJ software.

2.4 Reynolds Numbers

The Reynolds Number is a dimensionless parameter that is used to predict whether a flow rate will be laminar or turbulent. It is a ratio of the inertial forces and the viscous forces:

$$Re = \frac{VD}{\nu} \tag{2.7}$$

Where V is the flow velocity, D is the traveled length of the fluid, and ν is the kinematic viscosity.

In laminar flow, Re ≤ 2000, fluid particles move in a straight line, and will continue to move in a straight line until acted upon. In most microfluidic devices fluid flow will be laminar. The flow rate and dimensions of most microfluidic devices are too small for convective mixing to occur naturally, diffusion is the predominant mixing mechanism. The branching network of gradient generators helps disrupt the particle path, which results in diffusive mixing of the two species.

The work presented here examines a device consisting of 16 cell culture wells connected by a thin channel. The device consists of three layers: the cell culture network, a gradient generator, and an interdigitated electrode array for electrochemical impedance spectroscopy (EIS), shown in **Figure 2.4**. Using PDMS replica molding, the cell culture and gradient generator networks are imprinted into a PDMS mold, which is bonded on a glass substrate containing the electrode array.

This device uses a combination of electrical and optical methods to quantify and observe cellular systems. This novel device enables control over the cellular microenvironment.

With the gradient generator, 16 unique concentrations are developed from two initial concentrations, and the varying effects can be studied simultaneously.

3. METHODS

3.1 Traditional Cell Culture

All biological material was handled with proper aseptic and biohazard technique. Liquid biohazards were aspirated into a 10% bleach solution and disposed of following appropriate protocol. All solid waste was placed in a hard-sided biohazard container, and sharps were placed in a Sharps biohazard container.

NIH 3T3 mouse fibroblasts were cultured in tissue treated T-75 flasks. The basal media was Dulbecco's Modified Eagle Medium (DMEM) supplemented with 10% fetal bovine serum (FBS), 1% penicillin-streptomycin antibiotic, and .1% Fungizone. The cells were incubated at $37°C$, with a relative humidity of approximately 95%, and a CO_2 concentration of approximately 5%.

Prior to use, media and trypsin were submerged in a sterile water bath until reaching physiological temperature. Sterile phosphate buffer solution (PBS) was used at room temperature.

For experimental purposes, the cell-line was continuously maintained. The cells were passed at 75-90% confluency, approximately every two to three days. To passage, the flasks were removed from the incubator and placed in a sterile biological safety cabinet. The media was aspirated and the cells were rinsed with PBS to remove any excess media. 3 mL of trypsin was used to detach the fibroblasts. The flask was then observed under light microscopy for three to five minutes, or until most cells had detached. The trypsin was neutralized with equal parts media and manually mixed with a pipette-aid to ensure single-cell suspension. 4 mL of cell solution was evenly split into two T-75 flasks, one for continuous culture and one for microfluidic experimentation. The cells were

resuspended in 10 mL of media per flask and returned to the incubator. Excess cell solution was properly discarded following the biohazard protocol.

3.2 Microscale Cell Culture

The following methods are used for acquiring a cell solution for microfluidic experimentation. The same DMEM complete media as describe above was used in these processes. Ideally, flasks at 85-95% confluency were used to ensure dense seeding of the device. The same culture technique described above was also used for rinsing, trypsinization, and neutralization of the cells. A portion of the resulting cell solution was then passed into a 1 mL sterile cryovial and used for loading the device.

3.3 Device Fabrication

The microfluidic device was fabricated using an SU8 master mold that was fabricated in a Class 1000 cleanroom. The device was manufactured using traditional soft lithography techniques. Photoresist was deposited onto a [P]100 silicon wafer. A mask of the device was placed atop the silicon wafer and exposed to UV light. The mask is then removed and the photoresist dissolved, resulting in an SU8 master mold of the device. The master mold contained three devices. However, due to lift off of the photoresist, only two devices were manufactured from the mold.

Poly(dimethyl siloxane) (PDMS Sylgard® 184, Dow Corning Corporation) was used to create the mold of the device. PDMS was mixed in a 1:10 ratio of curing agent to base. 40g of base and 4g of curing agent were used for the fabrication of this device. PDMS was manually stirred for 10 minutes then degassed under a vacuum. The PDMS was then poured over the SU8 master mold, placed in an oven at $70\ °C$, and cured for at least 24 hours. An X-Acto knife was used to cut and carefully peel the PDMS mold from the

silicon wafer. The individual devices were then cut from the mold, yielding two independent microfluidic devices. The four inlets and one outlet of the device are punctured using a 23-gage blunt tipped dispensing needle. Scotch tape was then adhered to and removed from the mold side of the PDMS two to three times to remove any particulates.

A standard microscope slide, $75\ x\ 50\ mm$, was washed with ethanol, rinsed with water, and dried using a Chemwipe. As with the PDMS mold, Scotch tape is adhered to and removed from the surface of the slide two to three times to remove any particulates. Air plasma treatment[1], 10s at 300mTorr, is used to irreversibly adhere the PDMS mold to the glass slide. The device is placed back in the oven to cure for a minimum of four hours prior to use.

3.4 Equipment Sterilization

Initial experiments used 70% IPA and ethanol as primary sterilization methods. The device, tubing, cryovials, and any conical and dispensing tips were sprayed thoroughly with 70% IPA. The solution evaporated prior to use. Ethanol was washed through dispensing tips, tubing, and the device prior to experimentation.

An Instant Pot IP-DUO80 was used for steam autoclave sterilization. The devices were wrapped in aluminum foil and sealed shut with autoclave tape. The Instant Pot was filled with 100 mL of distilled water, a metal shelf was placed in the Instant Pot, and the aluminum foil pouches were placed on top of the shelf. The same process is used for the Tygon tubing, cryovials, and conicals. Dry samples were autoclaved for 30 minutes at

[1] This research also looked at the efficacy of oxygen plasma treatment as a means to promote adherent cell culture.

10.2-11.6 PSI and 115-116°C [21]. Including 'warm-up,' the devices remained in the autoclave for a minimum of 45 minutes. The chamber could be manually vented or allowed to vent over time.

After steam autoclaving, the device and tubing were rinsed with ethanol, both for sterilization and as a wetting agent to reduce bubble formation within the device. Dispensing tips were submerged in ethanol prior to use.

Sterile syringes were used for all experiments. Proper aseptic technique is followed to preserve sterility when connecting dispensing tips.

3.5 Device Stage

A 3D-printed polylactic acid (PLA) stage magnetically attached to the desktop microscope. Atop that rests an aluminum machined heating stage designed specifically for the dimensions of the device. Two long shafts were drilled on either side of the device platform for uniform heating. Two heating elements were inserted and secured, ensuring limited metal was exposed. A thermocouple was used to monitor the aluminum stage temperature. It was inserted and secured using packing tape within a small cut out located next to the device platform between the two heating elements. The heating elements were set to physiological temperature, 37°C, and the stage was preheated and allowed to equilibrate prior to use during an experiment, roughly 30 minutes.

3.6 Experiment Procedure

The methods below are divided into two parts, macroscale and microscale. The macroscale experiments highlight traditional cell culture techniques and procedures. The macroscale experiments were used to generate a baseline for NIH 3T3 fibroblasts morphology in culture conditions. The microscale experiments describe the development

of the protocol that was used to sterilize, seed, and obtain adherent cell culture in the microfluidic device presented.

3.6.1 Macro Scale Experiments

The following protocols outline the experimental designs used for the macroscale characterization of NIH 3T3 fibroblasts using tissue culture treated 6-well plates. These experiments were used to demonstrate 'normal' morphology of fibroblasts in culture and to gain an understanding of fibroblasts characteristics under various media conditions. Seven macroscale experiments were conducted in total, sufficient data was obtained from two experiments, experiments 2 and 7, the methods and results from which are discussed below.

3.6.1.1 Rhodamine 123

A Rhodamine 123 (Rh123) stock solution was created following a PromoKine protocol [22]. 0.4 mg Rh123 was dissolved in 1 mL of dimethyl sulfoxide (DMSO) to create 1 mM Rh123-DMSO stock solution. The stock solution was wrapped in aluminum foil to protect it from light and stored at $4°C$.

3.6.1.2 Cell Culture

NIH 3T3 fibroblasts were cultured in a T-75 flask. After reaching confluency using the methods described above, the cells were passed into a tissue treated 6-well plate and left overnight to adhere.

3.6.1.3 Macroscale Experiment 2

This experiment examined the expression of Rh123 under varying glucose concentrations. A 1:1000 Rh123 dilution factor was used. Three tissue culture media

were prepared: 1) regular DMEM complete, 2) glucose free DMEM complete and 3) a 1:1 solution of regular and glucose free DMEM Complete. 1 mL of 3T3 cell solution, with approximately 3×10^5 cells/mL, was passed into each well and 2 mL of the respective cell media was added to each well. Two wells were covered in regular DMEM, two covered with glucose free DMEM, and the remaining two wells were covered with 1 mL regular DMEM and 1 mL glucose free DMEM. The 6-well plate was then incubated overnight, these conditions are shown below in **Figure 3.1A**.

Using an analytical balance, 0.4 mg of Rh123 was collected then dissolved in 1 mL of DMSO. 6 μL of Rh123 solution was dissolved in 6 mL of regular DMEM and in 6 mL of glucose free DMEM. The wells of the plate were aspirated, rinsed with PBS, and aspirated again. Each well was incubated with the stain media matching the wells media glucose concentrations, these conditions are shown in **Figure 3.1B** below. The 6-well plate was placed back in the incubator for 45 minutes. After the time elapsed, the solution was aspirated, and the wells were imaged dry.

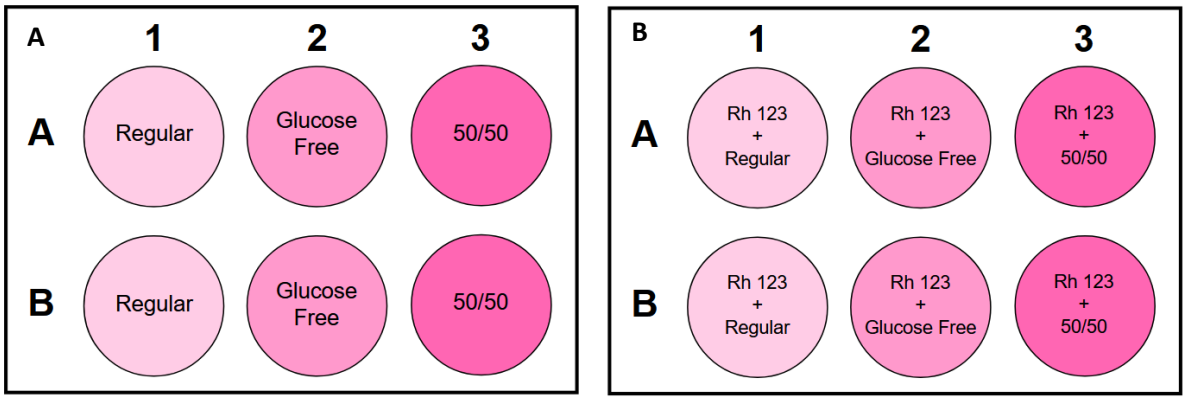

Figure 0.1 Macro Scale Experiment 2 Plate Map. Image A on the left shows the glucose concentrations used to culture NIH 3T3 Fibroblasts for 24 hours. Image B on the right shows the Rhodamine 123 and media type used for labeling and fluorescent microscopy.

3.6.1.4 Macroscale Experiment 7

This experiment sought to examine whether DMSO was causing detrimental changes to the cellular microenvironment. A 1:100 Rh123 dilution factor was used in this experiment. Using an analytical balance and weigh boat, two 0.4 mg samples of Rh123 were collected. For one solution Rh123 was dissolved in 1 mL of DMSO. The other solution was dissolved in of 1 mL of DMEM. 40 μL of each respective stain solution was dissolved in 4 mL of DMEM

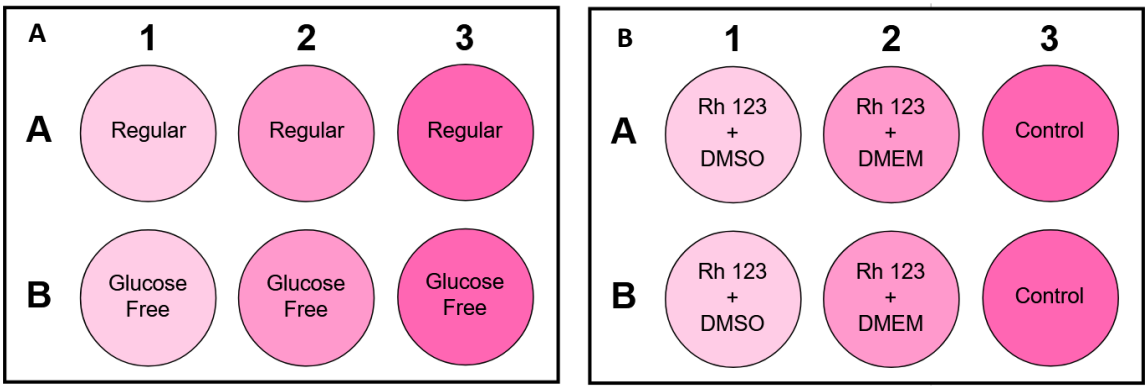

Figure 0.2 Macro Scale Experiment 7 Plate Map. Image A shows the culture conditions used to culture NIH 3T3 Fibroblasts overnight in a 6-well plate. Image B shows the three conditions tested for fluorescent microscopy.

NIH 3T3 fibroblasts were passed to a 6-well plate. Three wells contained 1 mL of cell solution and 2 mL of regular DMEM complete; the remaining three wells contained 1 mL of cell solution and 2 mL of glucose free DMEM complete, conditions are shown in **Figure 3.2** above. The plate was incubated overnight to allow for cell adherence. 2 mL of the DMSO stain solution was added to two wells, one from each media type, with one well acting as the control. The same set-up was followed using the DMEM stain solution. The cells were incubated for 45 minutes, the solution was aspirated, and 1 mL of PBS was added to each well. The wells were imaged wet.

3.6.2 Micro Scale Experiments

A 3D-printed polylactic acid (PLA) stage magnetically attached to the desktop microscope. Atop that rests an aluminum machined heating stage designed specifically for the dimensions of the device. Two long shafts were drilled on either side of the device platform for uniform heating. Two heating elements were inserted and secured, ensuring limited metal was exposed. A thermocouple was used to monitor the aluminum stage

temperature. It was inserted and secured using packing tape within a small cut out located next to the device platform between the two heating elements. The heating elements were set to physiological temperature, 37°C, and the stage was preheated and allowed to equilibrate prior to use during an experiment, roughly 30 minutes.

During Experiments 1-4 the heating stage was not functional, as a result these experiments were not conducted at physiological temperature. Successful use of the gradient generator was not achieved during any experiment due to lack of adhesion.

Table 3.1 below illustrates the key elements tested in each microscale experiment. Each experiment tested various conditions from sterilization methods, surface treatments, temperature, and seeding methodology. Experiments were grouped if they had the same experimental design and protocol. Each experiment is defined in further detail below the table.

Table 0.1 Outline of Micro-Scale Experiments. *The table below highlights key conditions tested for all microscale experiments: device prep, experiment temperature, surface treatments, seeding method, and perfusion.*

Exp. #	Device Prep	Temperature	Surface Treatment	Seeding	Perfusion
1 and 2	70% IPA DMEM	Room Temp.	Air Plasma	Syringe Pump Q= 0.01mL/hr	None
3, 4 and 5	70% IPA DMEM	Room Temp.	Air Plasma	Syringe Pump Q= 0.5 mL/hr	None
6	Ethanol PBS DMEM	Physiological Temp.	Air Plasma	Syringe Pump Q = 0.5mL/hr	None
7 and 8	Autoclave Ethanol DMEM	Physiological Temp.	Air Plasma	Syringe Pump Q = 0.5mL/hr	None
9	Autoclave Ethanol DMEM	Physiological Temp.	Air Plasma PLL- 2hrs 37C	Syringe Pump Q = 0.5mL/hr	Manual T= 120
10	Autoclave Ethanol DMEM	Physiological Temp.	Air Plasma PLL- 2hrs RT	Syringe Pump Q = 0.5mL/hr	Manual T = 150
11	Autoclave Ethanol Distilled H2O	Physiological Temp.	Air Plasma PLL- 2hrs RT	Vacuum Suctioned	None
12	Autoclave Ethanol Distilled H2O	Physiological Temp.	Oxygen Plasma Air Plasma PLL- 20min RT	Vacuum Suctioned	Manual T = 60 T = 120
13	Autoclave Ethanol Distilled H2O	Physiological Temp. Incubator over night	Air Plasma PLL - 15min 37C	Vacuum Suctioned	Manual T = 22 hr
14	Autoclave Ethanol Distilled H2O	Physiological Temp. Incubator over night	Air Plasma PLL - 2hrs RT H2O overnight	Vacuum Suctioned	Manual T = 24 hr

3.6.2.1 Microscale Experiments 1 and 2

For sterility, all experimental equipment was sprayed with a 70% IPA solution. Three medium length pieces of Tygon tubing were cut, sprayed with IPA, and connected to the inlet and outlet of the cell well channel and the outlet of the device. The free ends of the tubing connected to the outlets were placed in a 50 mL beaker and taped in place for waste collection. A 1 mL syringe containing ethanol was placed in a syringe pump and preset to a flow rate of 0.01 mL/hr. The dispensing tip was inserted into the Tygon tubing. The syringe was manually pushed to fill the length of the tubing with ethanol before the syringe pump was turned on to flush the device. The device was sterilized with ethanol for at least 10 minutes, after which a syringe with 1 mL of DMEM complete was connected and flushed through the device. While the device was being rinsed with media, NIH 3T3 fibroblasts were being passed from a T-75 flask into a sterile conical. The cell solution contained 3 mL of cell solution and 3 mL of trypsin. A sterile syringe was used to collect 1 mL of cell solution, then connected to the device, and secured in the syringe pump. The pump remained on for 30 minutes. The syringe and tubing were disconnected from the inlet of the device, and the device was left untouched for five minutes prior to imaging.

3.6.2.2 Microscale Experiments 3-5

The general protocol described above was implemented for the three following experiments, with some exceptions. The device was flushed with IPA at a flow rate of 0.04 mL/hr for approximately 10 minutes, followed by DMEM complete media for a

minimum of 10 minutes at the same flow rate[2]. The cell solution was collected the same way as described in Experiments 1 and 2, but prior to introduction to the device, the solution was manually mixed using a micro-pipette to ensure a single cell suspension. The solution was then introduced into the device using the syringe pump with a flow rate of 0.5 mL/hr for 10 minutes. After cell perfusion, all tubing was removed from the device, except the outlet. Using sterile tubing, the inlets and outlets of the gradient generator and cell well channel were closed off. The devices were imaged until bubble formation compromised the majority of the wells.

3.6.2.3 Microscale Experiments 6[3]

The heating stage was assembled, turned on, and allowed to pre-heat prior to use. The device was flushed with ethanol at 0.05 mL/hr for 10 minutes, followed by phosphate buffer solution (PBS), then media, each for 10 minutes at 0.5 mL/hr. The cell solution was then introduced at 0.5 mL/hr for five minutes. The syringe pump was then turned off and disconnected from the device. Then the wells were imaged for the duration of the experiment.

3.6.2.4 Microscale Experiments 7 and 8

These experiments looked at the shelf life of the devices to examine whether the hydrophobic nature of PDMS after plasma treatment effected adherent cell culture within the device. For both experiments, the devices were used immediately following a four-

[2] It is important to note, for the fourth experiment a second device was prepped after multiple bubble formation in the initial device. Due to time constraints (cell viability), the second device was used directly from clean room fabrication and was not sterilized using IPA but was flushed with media before cell introduction. The same cell solution was used for both devices at roughly the same time.
[3] Autoclaved devices and equipment were used for all experiments from this point forward.

hour cure period after air-plasma treatment. The devices were then autoclaved for 30 minutes.

The heating stage was set up, sterilized using 70% IPA and preheated while the device was autoclaved. Once removed from the aluminum foil, the device was placed in the heating stage. The syringe pump was set to 0.5 mL/hr to flush the cell well channel with ethanol, followed by media, for a minimum of five minutes to ensure the device was completely flushed with both fluids and all ethanol was removed prior to introducing cells. Simultaneously, the inlets to the gradient generator were manually flushed with ethanol, followed by media. Visual inspection was used to ensure all excess ethanol was rinsed from the device. The outlet tubes were inspected for the presence of media, evidenced by its pink color. The phenol red in the media changes color as the pH changes, the pink color observed highlights an increase in pH of the media. Media syringes were left connected to the inlets of the gradient generator to limit bubble formation and for media perfusion later on in the experiment. The cell solution was introduced using the syringe pump at a flow rate of 0.5 mL/hr for five minutes. The syringe and tubing were disconnected from the inlet of the cell well channel.

3.6.2.5 Microscale Experiment 9

Based on experiments 7 and 8, the shelf life, or time between plasma treatment and use, was continued to be examined during this experiment. This device cured in the oven after plasma bonding for approximately 24 hours before being autoclaved. The device was manually flushed with ethanol, then connected to the syringe pump, and washed with distilled water at 0.5 mL/hr.

A new syringe was filled with ~0.5-mL of Poly-L-Lysine solution (0.01%) (PLL) from EMD Millipore Corp. and manually introduced through the cell well channel of the device. Once all 16 wells were filled with PLL, the device was placed on the heating stage and incubated for two hours. Directly following incubation, the device was flushed with 1 mL of distilled water, and then connected to the syringe pump and washed with media at 0.5 mL/hr until pink fluid was present in both outlet tubes. Following the same protocol described above, the cells were introduced to the device. Using a 1 mL syringe filled with media and connected to the device, manual fresh media perfusion was attempted through the cell well channel after 120 minutes.

3.6.2.6 Microscale Experiment 10

For this experiment, the device was incubated with PLL for two hours at room temperature. The rest of the procedure for this experiment followed the same protocol described above in Experiment 9. Media perfusion was manually perfused through the cell well channel after 150 minutes of cell incubation.

3.6.2.7 Microscale Experiment 11

A new protocol was developed for this experiment. The goal was to examine a different loading technique that mitigates possible shear stress on the cells when using a dispensing tip and limits bubble formation.

The device was plasma treated and autoclaved 24 hours prior to use.

The device was manually washed with ethanol and rinsed with distilled water before being loaded with PLL. The device was incubated with PLL for two hours at room

temperature prior to use. Following incubation, the device was flushed with media to remove all excess PLL.

The cell solution was collected and dispensed into a sterile 1 mL cryovial and placed upright in a cryovial holder. Clean tubing was connected to the inlet and outlet of the cell well channel. The outlet tubing was connected to an empty 1 mL syringe affixed with a dispensing tip. The inlet tubing was carefully inserted into the cryovial, such that the tubing was resting on the base of the cryovial and fully submerged in fluid. The syringe attached to the outlet was slowly pulled, creating a vacuum that slowly filled the device. Once the device was fully loaded, the tubing was disconnected and the wells were imaged.

3.6.2.8 Microscale Experiment 12

The efficacy of air plasma bonding on adherent cell culture was compared to a device fabricated using oxygen plasma bonding in this experiment. Everything else about the two devices remained constant throughout the course of this experiment.

The devices were autoclaved, flushed with ethanol, and then rinsed with distilled water prior to a 20-minute PLL incubation at room temperature. The devices were then flushed with media. Due to bubble formation, liquid was suctioned from both devices and the devices sat dry while the cell solution was prepped. 1 mL of cell solution was obtained and pipetted into a cryovial. New tubing was connected to the inlets and outlets of the cell well channel of both devices. The devices were then loaded as described in Experiment 11. Media was manually was perfused through the cell well channel at 60 and 120 minutes.

3.6.2.9 Microscale Experiments 13 and 14

This experiment is the first attempt at long term experimentation and utilizes the finalized loading protocol for the device.

For Experiment 13, a 1 mL pipette tip container was used for long term culture within a sterile incubator. The container was autoclaved for 30 minutes and transported to a sterile biological safety cabinet before the aluminum foil was removed. Sterile distilled water was poured into the base of the container to create a humid environment. After loading the device, it was placed on the pipette tip rack within the container. The container was shut and placed into the sterile incubator overnight.

For Experiment 14, the same 1 mL pipette tip container was used. However, the 1 mL tip rack was removed and replaced with a smaller gage tip rack with hopes of promoting sufficient gas exchange. Both pieces were placed in an autoclave for 30 minutes and transported to a biological safety cabinet before being opened to preserve sterility. A small amount of sterilized, distilled water was poured into the base of the container, and the loaded device was placed on the rack. The container was shut and placed within the sterile incubator overnight.

For both experiments, the following protocol was used to load the device. The device was sterilized in an autoclave for 30 minutes. The device was manually flushed with ethanol and distilled water before PLL was introduced. The device was filled with PLL and incubated for 15 minutes at physiological temperature before being flushed with distilled water followed by media. A sterile syringe was filled with 0.5 mL of media and connected to a dispensing tip and Tygon tubing. Care was taken to limit bubble formation within the syringe. Media was manually dispensed to fill the length of the tubing with

media. The tubing was then inserted into a cryovial containing cell solution. Once the tubing was fully submerged in the fluid, ~0.01 mL of cell solution was suctioned into the tubing. Gently, the syringe was pushed creating a bubble at the tip of the tubing, which was then inserted into the device, forming a wet-connect. The 0.01 mL of cell solution was then manually introduced into the device. All tubing was disconnected from the device, except for the main outlet. Two short pieces of tubing were cut and filled with media. One tube was used to connect the inlet and outlets of the cell well channel via a wet-connect and the other was used to connect the inlets of the gradient generator. Initial images of all 16 wells were taken. The device was then placed in the sterile tips container and placed in an incubator overnight. After a 22-hour incubation, the device was removed, imaged, and perfused manually with fresh media before being placed back in the incubator for 48 hours.

For Experiment 14, two devices were prepped and used. The devices were autoclaved and rinsed as described above. The PLL sat in the device for two hours at room temperature and rinsed with water. The devices were filled with distilled H_2O and sat overnight. The following day, the devices were rinsed with media and loaded with cells, using the same method as described above. The devices were imaged and then the inlets and outlets were closed off using tubing filled with media. The devices were then placed within the new sterile tips container and placed in the incubator for 24 hours.

3.6.2.10 Clean-Up

Proper biohazard protocols were followed during the cleanup for all experiments. Any single use equipment that came in contact with biologics was disposed of in a hard-sided biohazard container. Any liquids were placed in a liquid biohazard disposal container

containing a 10% bleach solution. Any re-useable equipment was washed with a 10% bleach solution. Counter tops, microscope, and any other equipment or surface that came in contact with biologics were sprayed and wiped down with a 70% IPA solution.

3.7 Imaging Methodology

3.7.1 Macro Scale

A widefield fluorescence microscope was used for macroscale cell culture imaging. A Fluorescein isothiocyanate (FITC) fluorescence was used to observe Rhodamine 123 concentration within the cells. The fluorophore in Rhodamine 123 absorbs blue light, 505 nm, and emits green light, 534 nm [22]. Excitation was provided by a mercury arc lamp source filtered using a FITC-specific filter cube.

Tissue treated 6-well plates seeded with NIH 3T3 fibroblasts were imaged. The cells were rinsed with PBS after staining, aspirated, and then a thin layer of PBS was added to each well for imaging. A 10X objective was used. Multiple images were taken per well: first a white-light photo, followed by a fluorescence photo of the same frame. Care was taken to limit photo bleaching. The black and white images were then stacked with the fluorescent image using ImageJ software, see **Image 4.1** and **Image 4.2** below.

3.7.2 Micro Scale

A LabSmith SVM400 epifluorescence and brightfield microscope was used to image cells within the microfluidic device and to monitor cell behavior throughout the course of an experiment. The microscope software had the ability to set and save specific locations on the microscope stage, denoted A-J. Once the device was fixed to the stage, the 16 wells were manually examined for the presence of cells. Five wells per side were imaged,

and the respective location saved. Images were then recorded every 30 minutes for the duration of the experiment.

The images were processed using NIH ImageJ software. Cells were manually counted using the cell-counter plug-in and recorded in Microsoft Excel.

4. RESULTS

4.1 Statistics

Cell count data obtained from ImageJ Cell-Counter was recorded in Microsoft Excel. Due to large variations in results from experiment to experiment, only experiments that lasted a minimum of 90 minutes (n =3) with a minimum of three wells (n=3) were analyzed. Based on that criteria, only Experiments 3, 4, 5, 6, and 10 generated sufficient data points.

4.1.1 Analysis of Cell Count over Time

Preset locations, denoted A-J, were used to record images at 30-minute intervals throughout the life of an experiment. Using NIH ImageJ software, the cells were manually counted and recorded in Microsoft Excel. The average and standard deviation of cells present in the device at each time interval was calculated. Using Minitab statistical software, an analysis of variance with Tukey simultaneous tests for differences of means and basic summary statistics were reported. The results of these analyses are shown in **Figure 4.3** and **Figure 4.4** below.

4.1.2 Analysis of Seeding Density as a Function of Distance

Preset locations were used to record images throughout the duration of an experiment. Locations for imaging were chosen based on optical clarity (focus) and dense presence of cells. Ideally, five wells per side of the cell network were imaged. This sought to look at whether a trend exists between the loading pattern of the device and subsequent distribution of the cells throughout the device.

The average cell count in each well for the duration of the experiment was calculated using Microsoft Excel. From there, the data sets were transferred to Minitab, where a

Graphical Summary was generated for each experiment. The basic summary statistics were collected and analyzed for any trends. An analysis of variance (ANOVA) with Tukey simultaneous tests for differences of means was also reported. The results of these analyses are shown in **Figure 4.6** and **Figure 4.7** below.

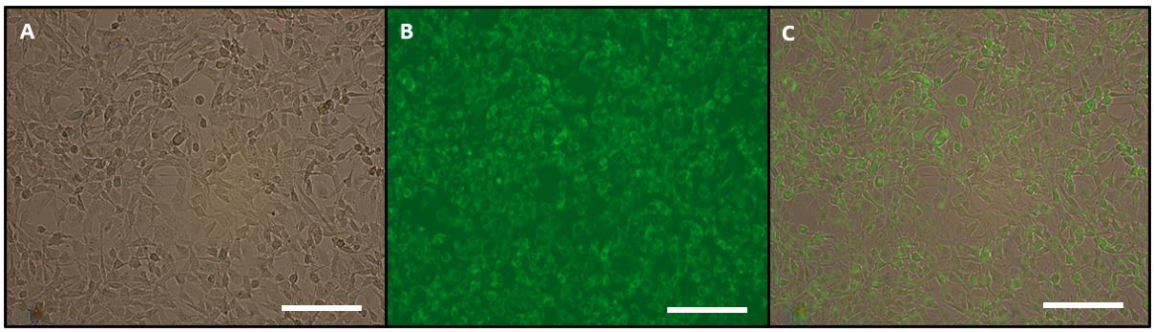

Figure 0.1 Glucose Free Macroscale Fibroblast Culture: Adherent cell culture of fibroblasts cultured in glucose free media for ~24 hours. Phase contrast imaging (A), fluorescent microscopy (B), Images A and B stacked using NIH ImageJ software (C). Scale bar represents 1000 μm.

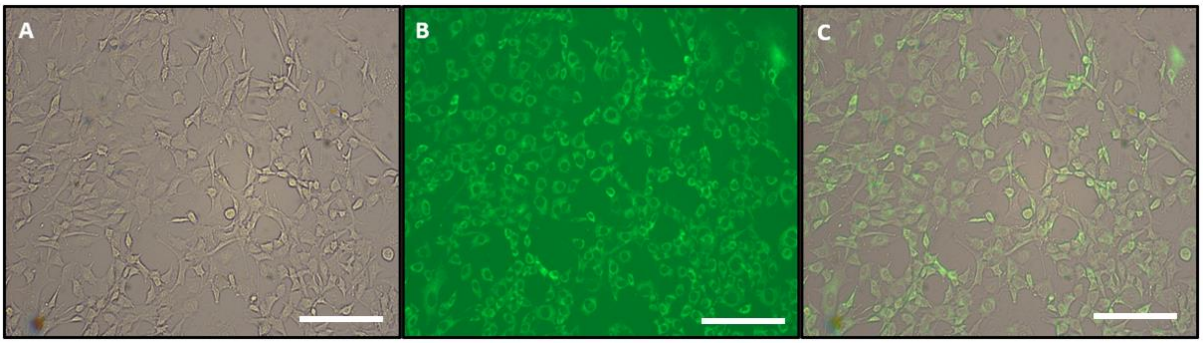

Figure 0.2 Macroscale Fibroblast Culture in a 6-well Plate: Adherent cell culture of fibroblasts, cultured in regular DMEM media for ~24 hours. From left to right: phase contrast (A), fluorescent microscopy (B), images stacked using NIH ImageJ software (C). Scale bar represents 1000 μm.

Figures 4.1 and **4.2** examine the accumulation of Rhodamine 123 in the mitochondrial membrane of NIH 3T3 fibroblasts when cultured in media supplemented with varying amounts of glucose. These images provide characteristic images of fibroblast culture at the macroscale that this work sought to recreate at the microscale.

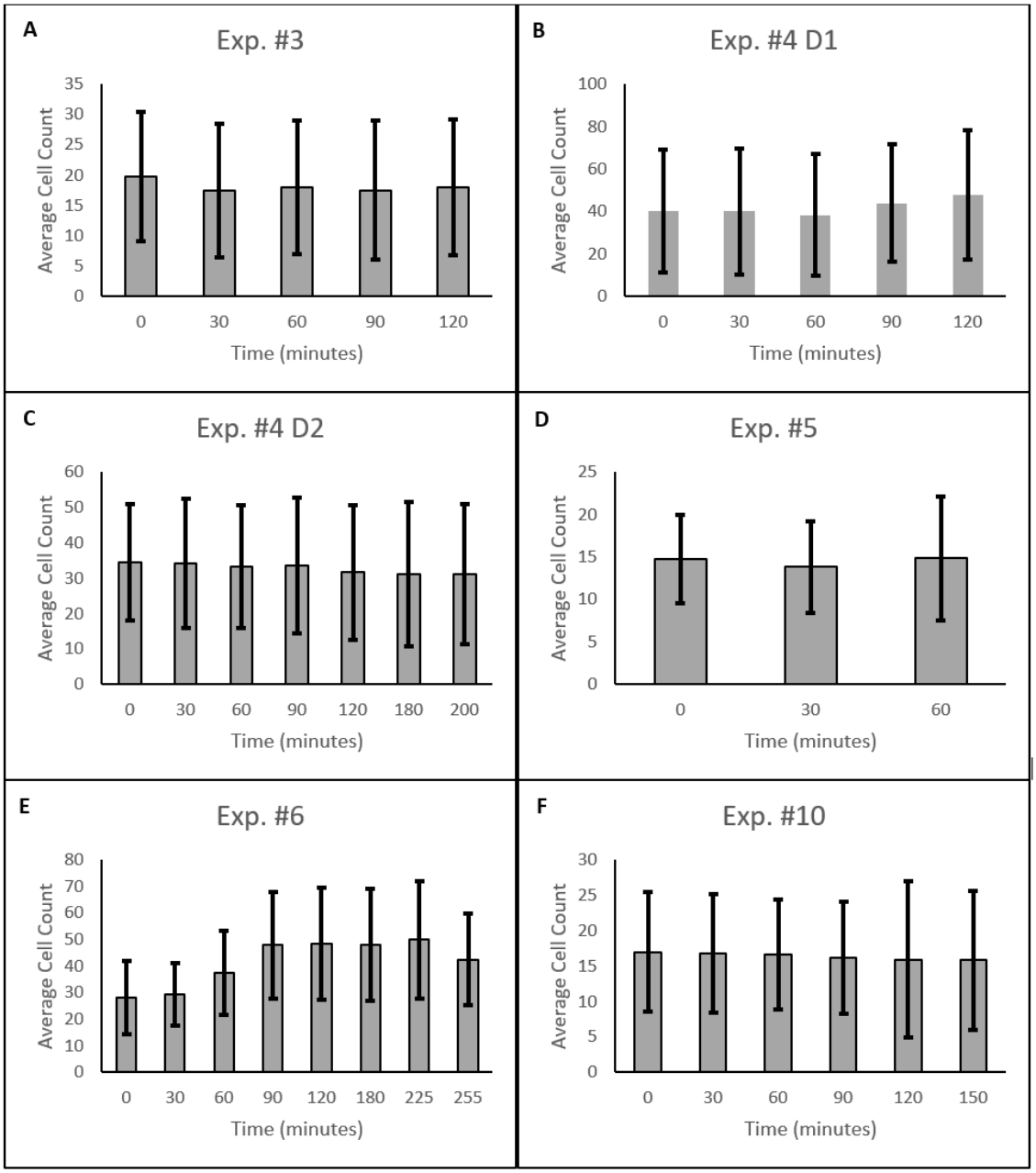

Figure 0.3 Average Cell Count as a Function of Time: Figures A-F show the average cell count across the entire device for the duration of each respective experiment. Cells were counted manually using NIH ImageJ software and recorded in Excel. Average and Standard Deviations were calculated in excel.

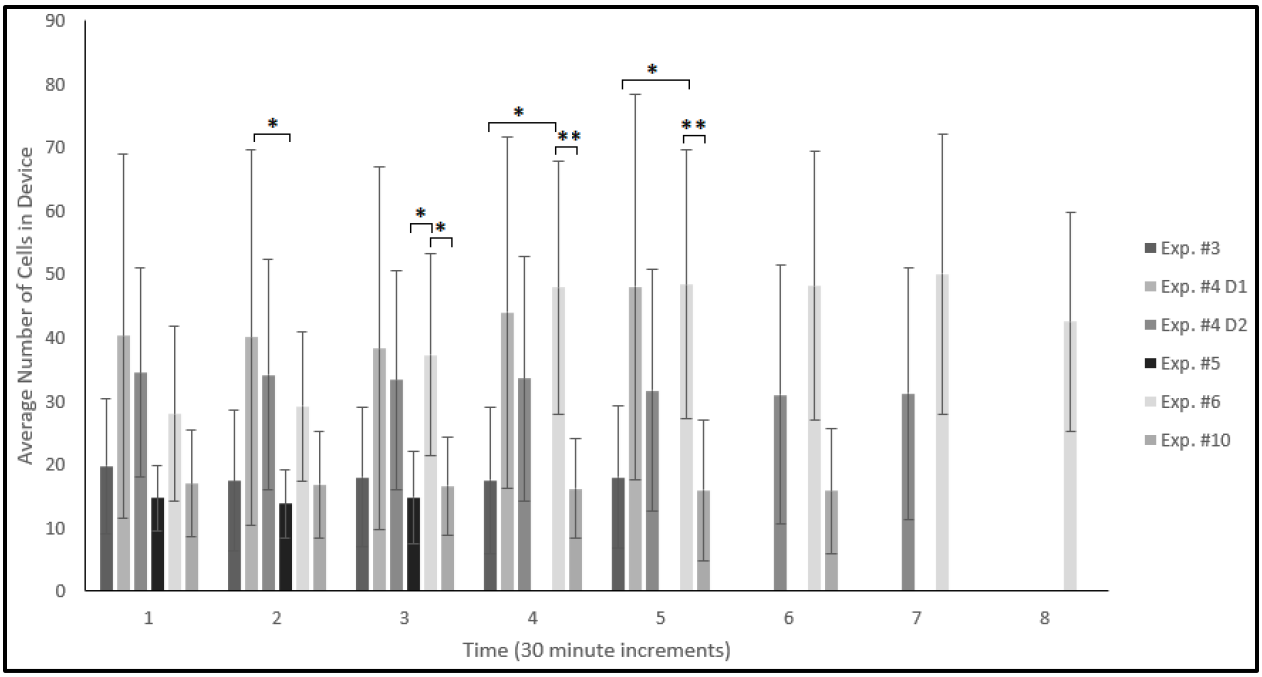

Figure 0.4 Average Cell Count in the Device as a Function of Time per Experiment: This bar chart examines the average number of cells in the device over time for all experiments that lasted a minimum of 90 minutes. Each point along the x-axis represents thirty minutes. * denotes a p value below 0.05. ** denotes p-value below 0.01

Based on Tukey Tests, after 30 minutes, a statistical difference with a p-value of 0.047 was observed between Experiments 4 and 5. After 90 minutes, a statistical difference was observed between Experiments 5 and 6, and Experiments 10 and 6 based on a p-value of 0.034 and 0.03 respectively. After 120 minutes, a significant difference was observed between Experiments 3 and 6, and Experiments 6 and 10, with p-values of 0.012 and 0.002, respectively. After 150 minutes, a significant difference was observed between experiments 3 and 6, and Experiments 6 and 10, with p-values of 0.018 and 0.002, respectively. However, due to large variations in experimental designs it is difficult to accurately compare between experiments.

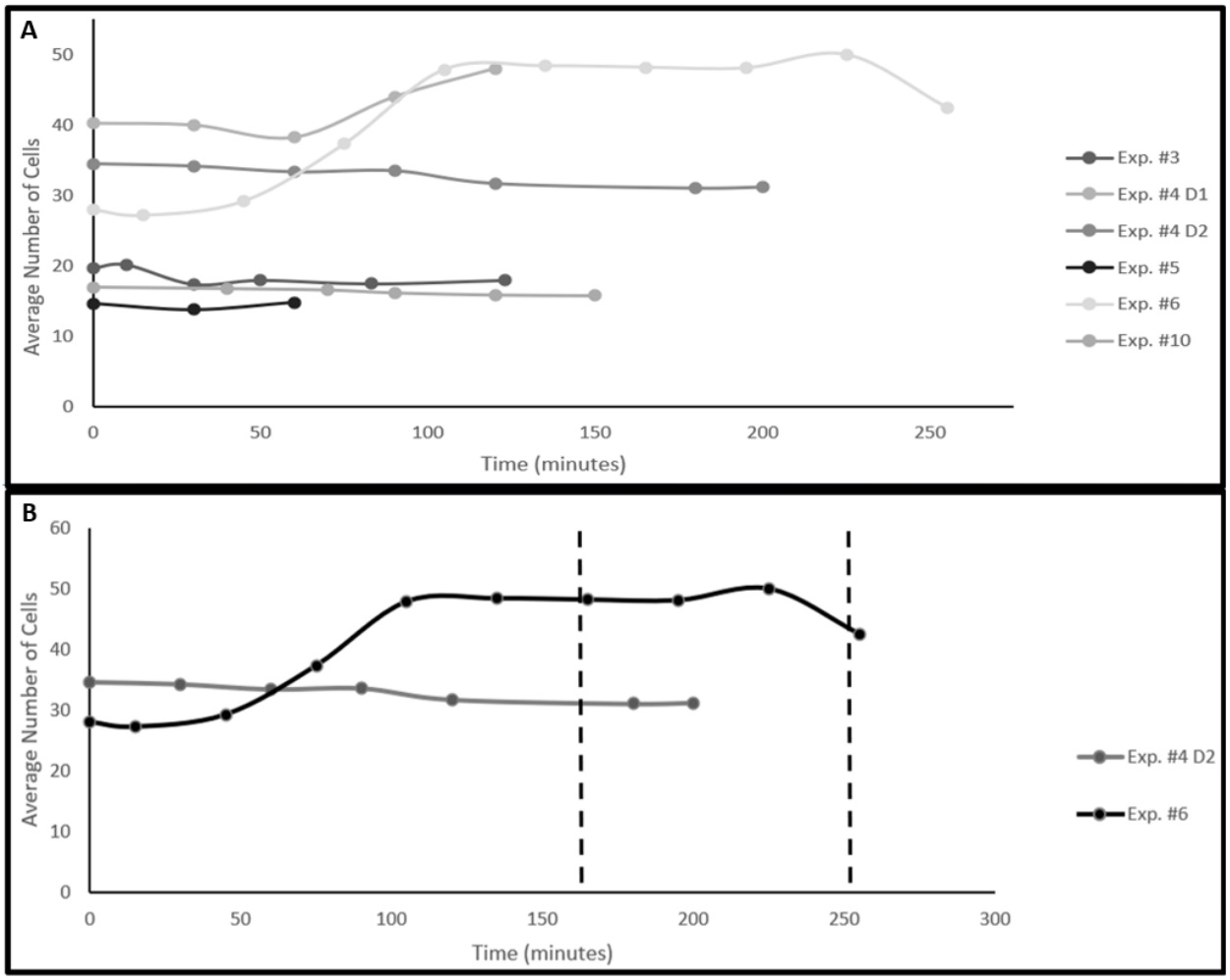

Figure 0.5 Examining the Effective Culture Time of the Device. Figure A is a smooth line curve of the average cell count in the device per experiment over time. Figure B highlights the two experiments Experiment 4 device two and Experiment 6. The dashed lines represent the expected time period when the nutrients in the media are depleted.

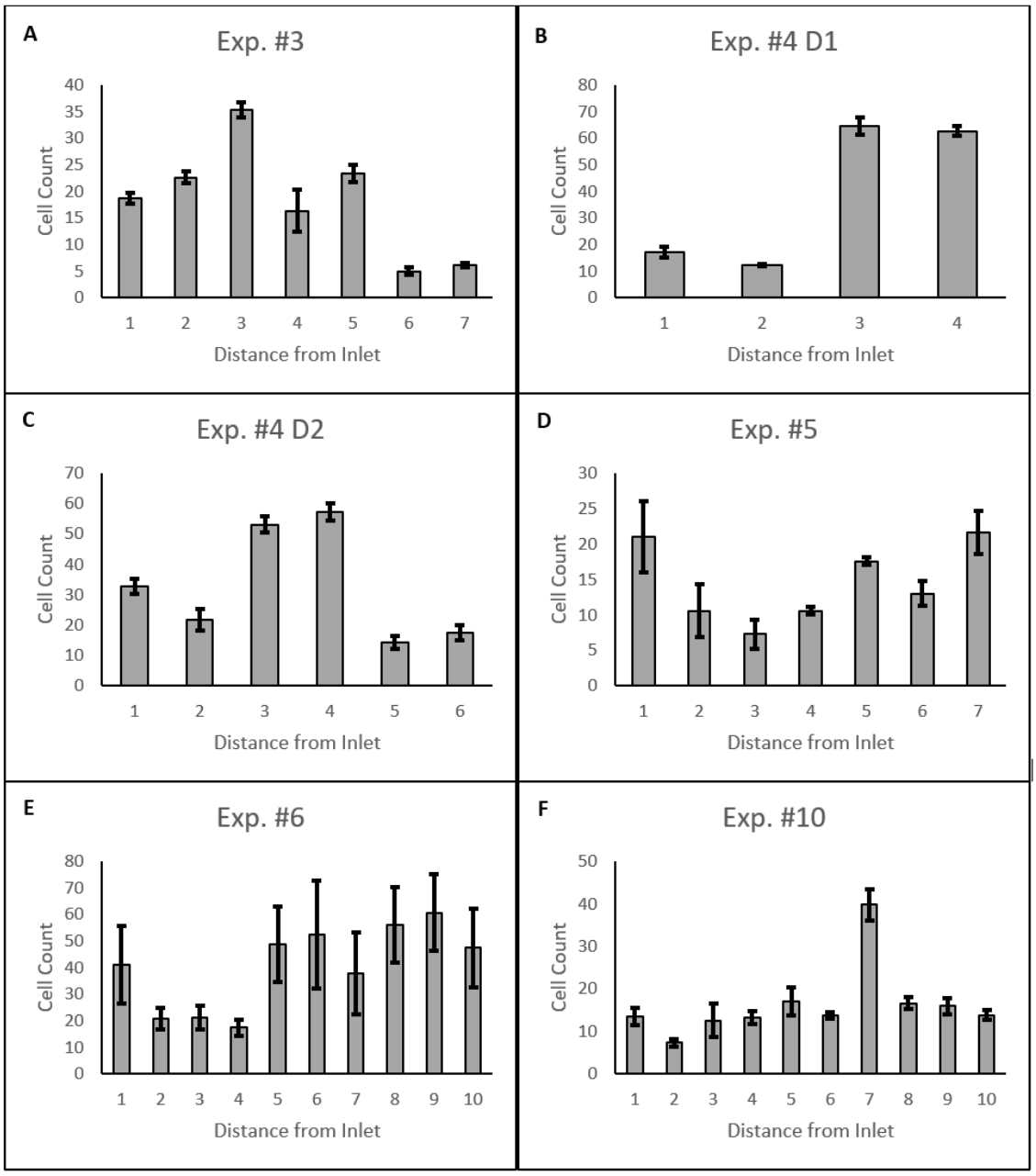

Figure 0.6 Cell Count as a Function of Distance: Figure A-F are bar graphs of the average cell count per well as a function of distance. The distance from the inlet is represented on the x-axis, with 1 representing the well closest to the inlet and imaged first.

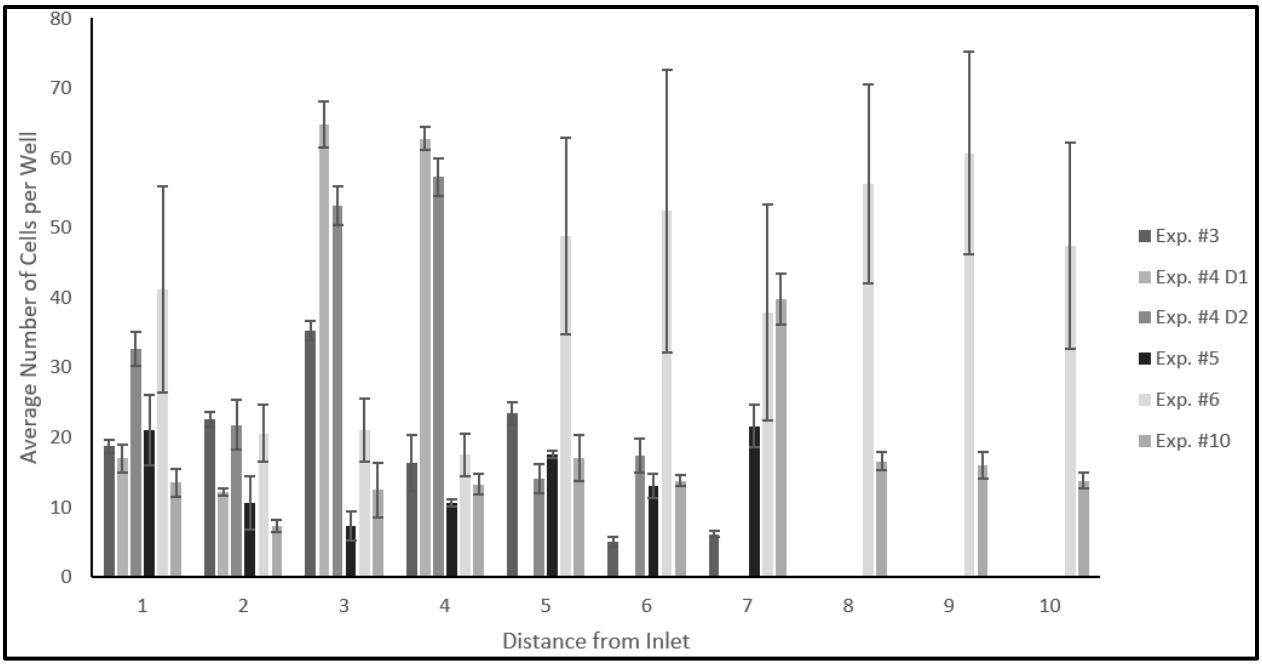

Figure 0.7 Average Number of Cells as a Function of Distance for each Experiment: This bar plot examines the average number of cells per well as a function of distance, with 1 representing the image closest to the inlet and 10 the furthest.

It is important to note, while '1' represents the first well imaged closet to the inlet for each specific experiment, it is not always the same well across all experiments. After multiple ANOVAs were conducted on the data and Tukey Simulations were examined, a 'statistical difference' was observed between almost every experiment in every well. This data provides insight into the variability of the different loading techniques per experiment and could also highlight the variability in confluency of the flasks used to obtain the cell solution. However, due to the large variations in experimental designs it is difficult to accurately compare between experiments.

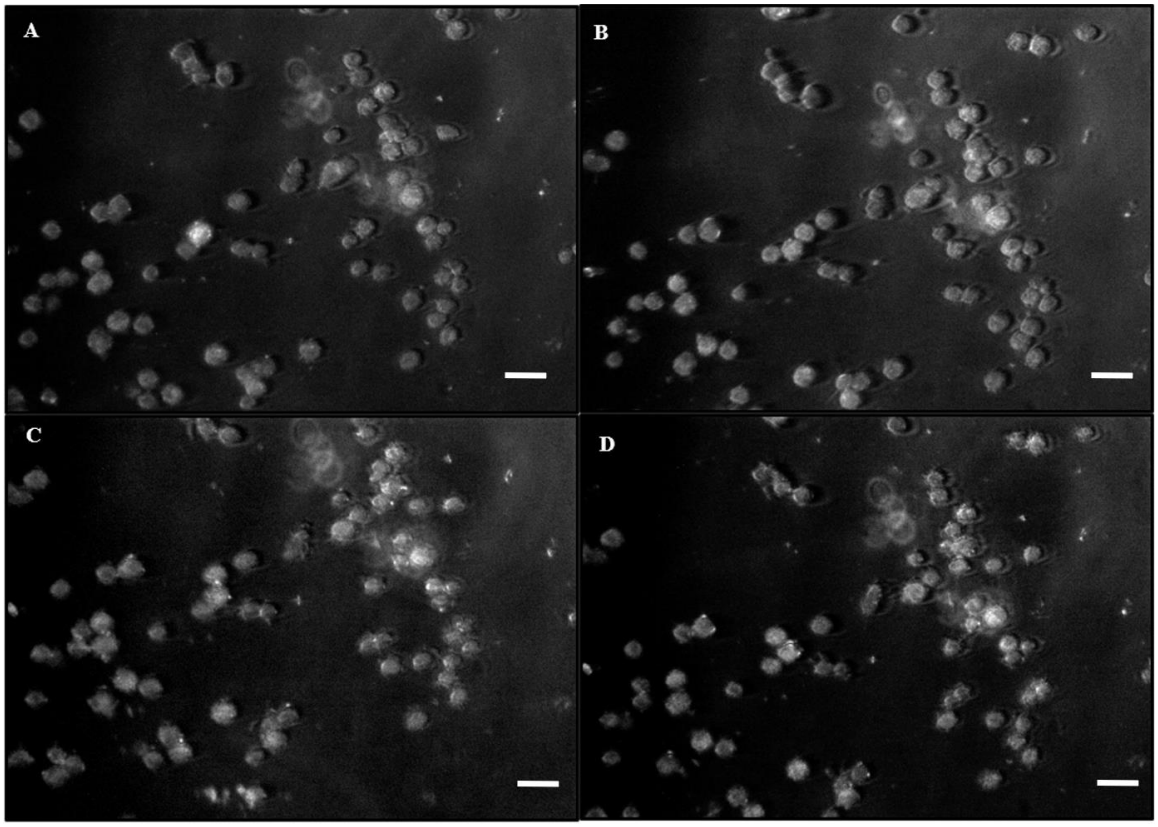

Figure 0.8 Experiment 4 Device 1 Culture Over time: Bright-field reflected light was used to obtain the above images. Time increases from left to right, top to bottom. A is imaged at t=0, B imaged at t=30 minutes, C imaged at t=60 minutes, and D imaged at t= 90 minutes. Scale bar represents 250 μm.

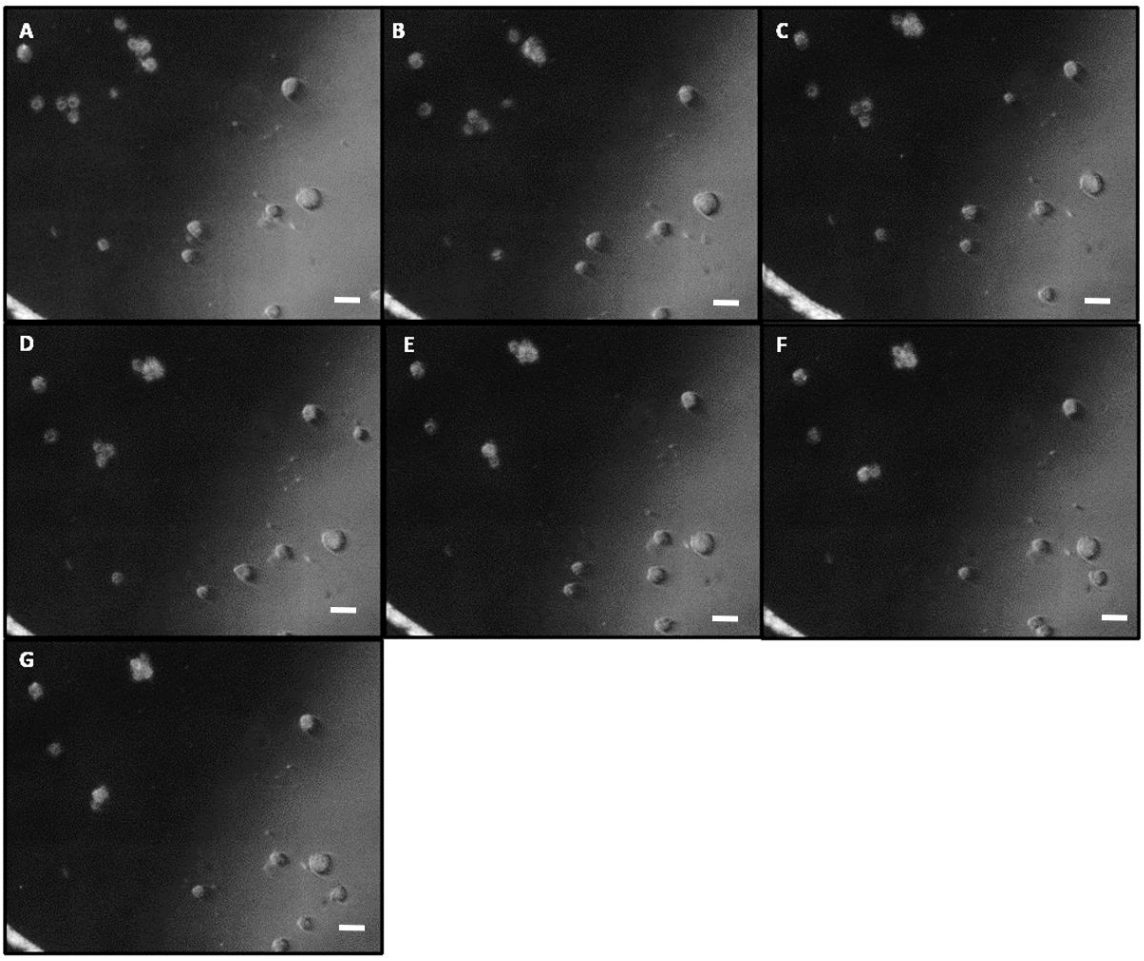

Figure 0.9 Experiment 4 Device 2 Culture over Time. Bright-field reflected light was used to obtain the above images. Time increases from left to right, top to bottom. Figures A-G were taken at approximately 30-minute intervals with the final image being recorded after 200 minutes (G). Scale bar represents 250 μm.

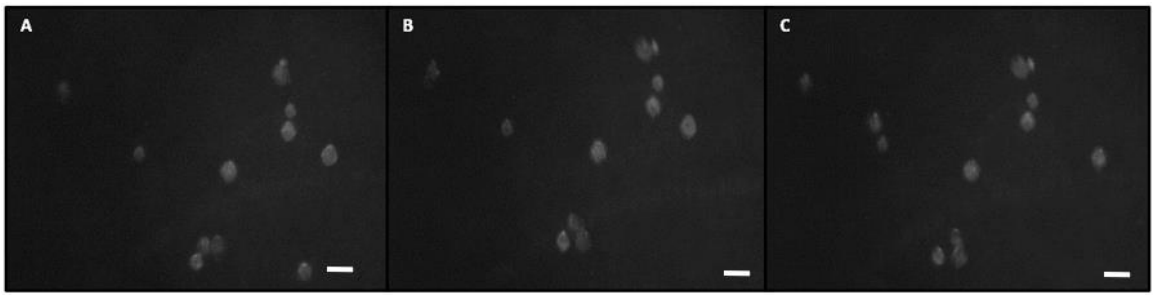

Figure 0.10 Experiment 5 Culture over Time: Bright-field reflected light was used to obtain the above images. Time increases from left to right. Images A-C were taken at 0, 30, and 60 minutes, respectively. Scale bar represents 250 μm.

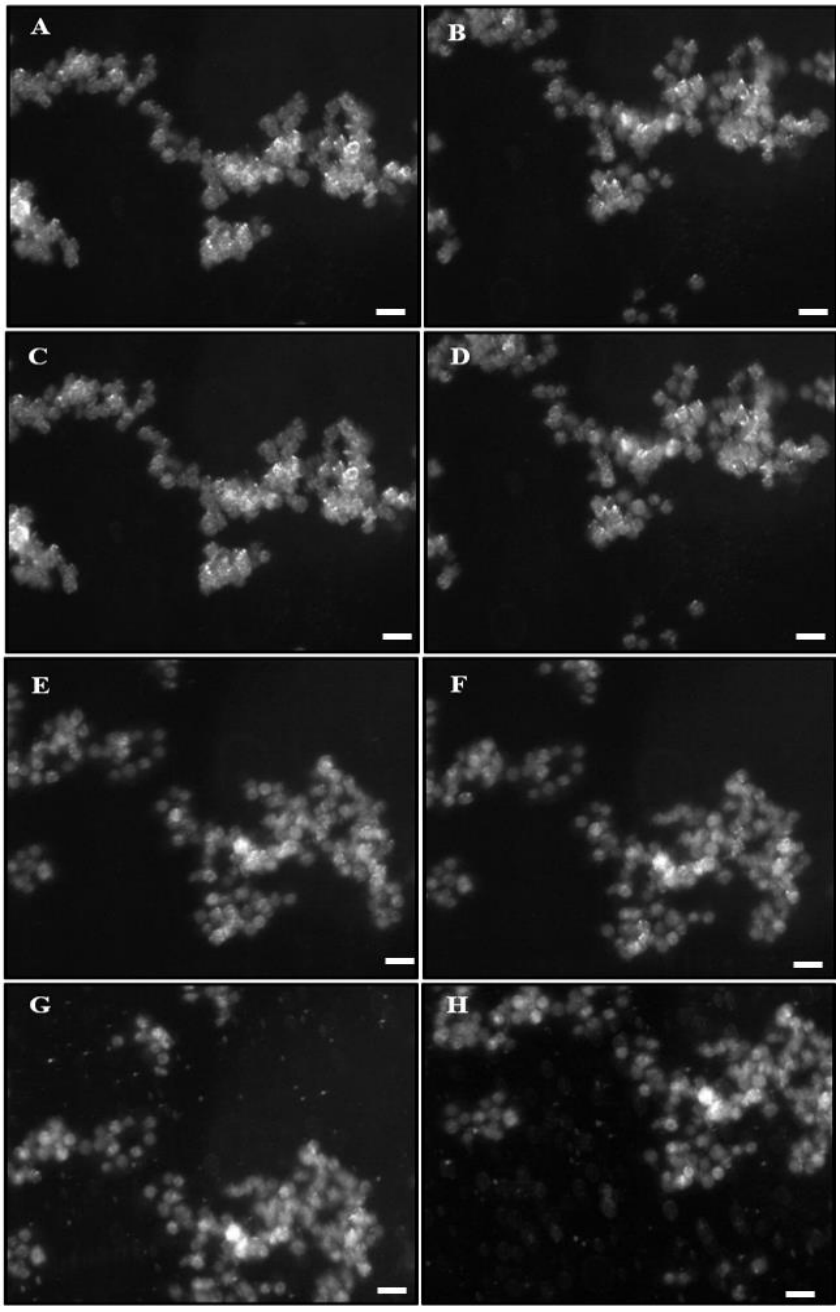

Figure 0.11 Experiment 6 Culture over Time: Bright-field reflected light was used to obtain the above images. Figures A-H were taken at 30-minute increments with the final time point being 200 minutes for Image G. The final image was taken after 255 minutes. The cells remained in suspension, but debris becomes noticeable after 180 minutes without perfusion. Scale bar represents 250 μm.

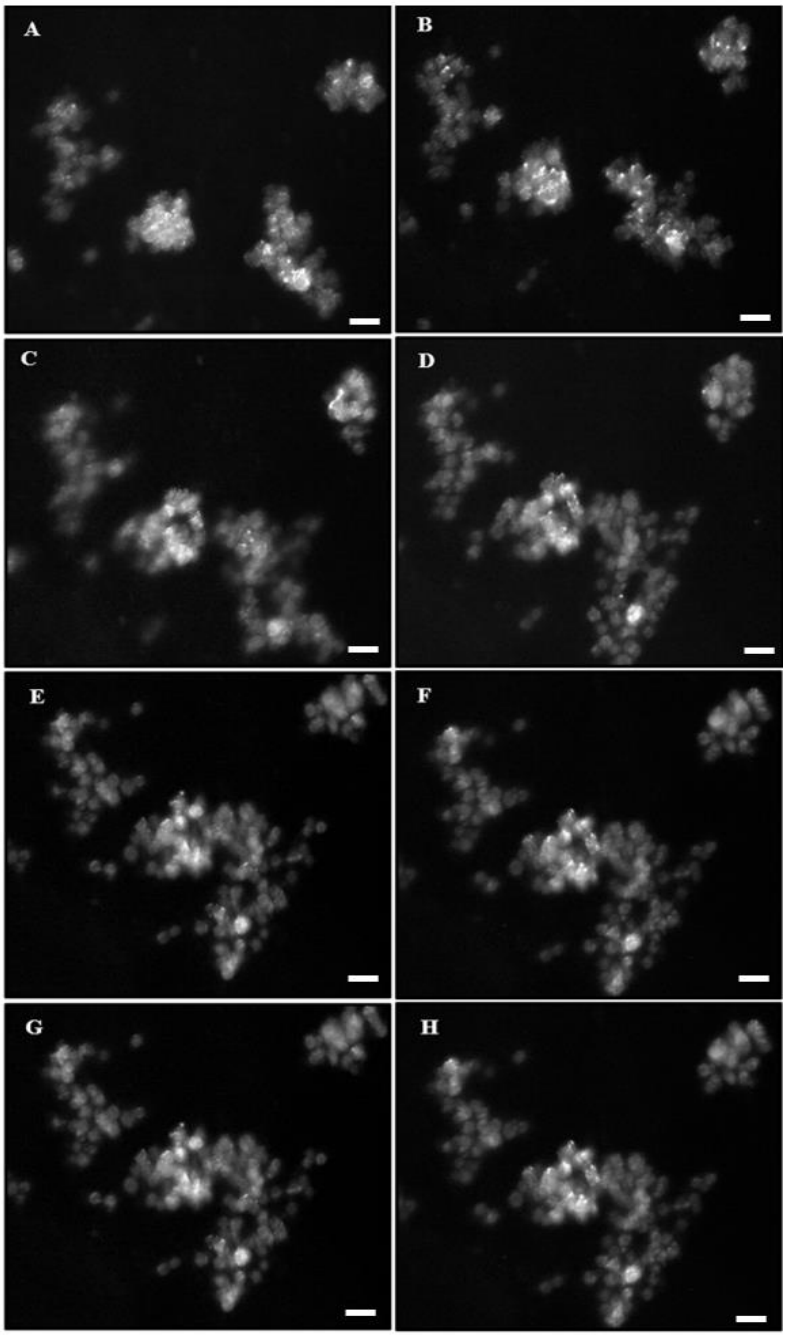

Figure 0.12 Experiment 6 Culture over Time: Bright-field reflected light was used to obtain the above images. Figures A-H were taken at 30-minute increments with the final time point being 200 minutes for Image G. The final image was taken after 255 minutes. The cells remained in suspension for the duration of the experiment, never adhering within the device. Scale bar represents 250 μm.

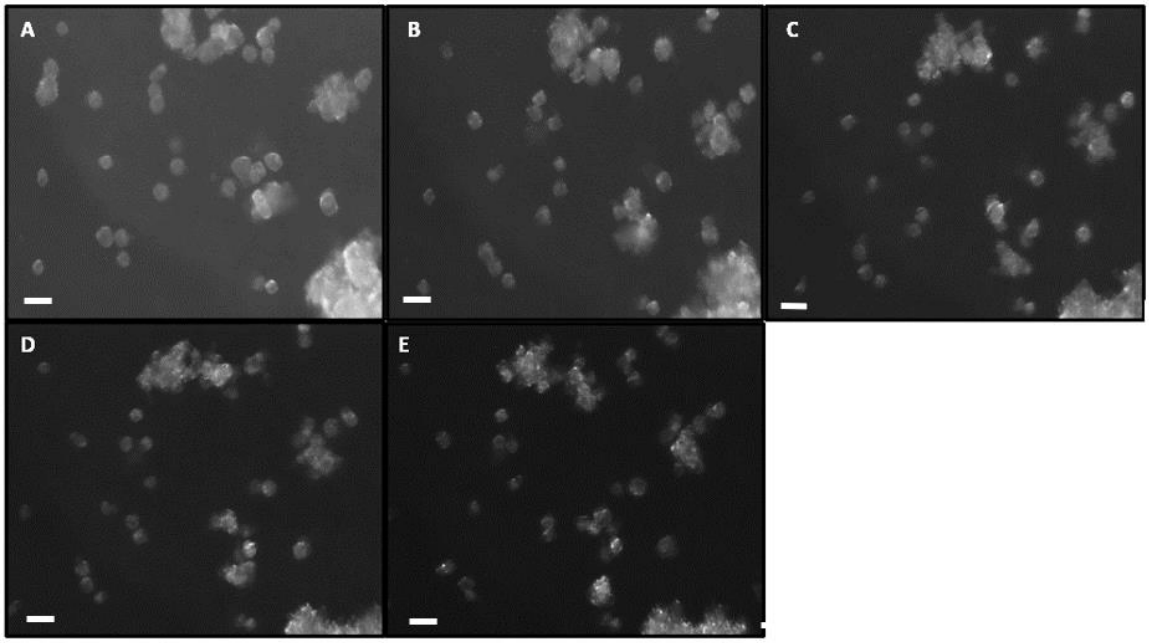

Figure 0.13 Experiment 10 Cell Culture over Time: Bright-field reflected light was used to obtain the above images. Images A-E were taken at 30-minute time intervals, with the final image being obtained after 120 minutes (E). Scale bar represents 250 μm.

Figures 4.8-4.13 show murine derived NIH 3T3 fibroblasts remaining in suspension throughout the duration of experiments, without any adherence to the surface. Possible adhesion was observed in **Figure 4.14** below. The cells remained adhered to the surface during constant perfusion for over 100 minutes.

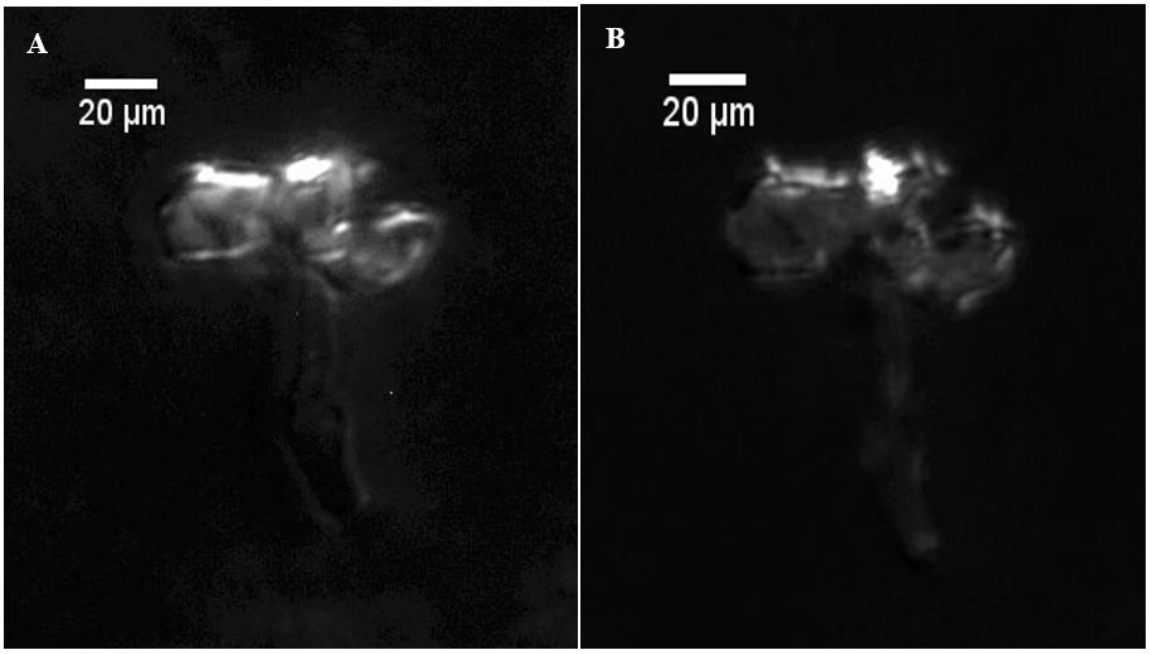

Figure 0.14 Adherent Cell Culture within the Device Experiment 12: Adherent cell culture was observed in the device after 60 minutes, shown in figure A. Figure B shows the cell after 176 minutes with intermittent media perfusion. Bright-field reflected light was used to obtain the above images.

5. DISCUSSION

An outline of the various conditions tested for each experiment is shown in **Table 3.1** above. The initial round of microscale experiments, Experiments 1-3, looked at directly translating macroscale culture techniques to microscale techniques. The end results showed no adherent cell culture and few if any cells were successfully introduced into the device. The first experiment used the initial device design that had larger cell wells, increasing the frequency and detriment of bubble formation within the device. The remaining microscale experiments were conducted using the second version of the device, where the most notable change was smaller well size. The changes made in later experiments focused on a) densely seeding the device and b) creating a suitable environment for cellular adhesion. Each experiment saw changes in loading techniques, with the goal of finding the method to best uniformly seed the device while limiting any possible shear stress on the cells. A sufficient number of cells need to be in each well in order for the necessary biochemical and biomechanical signaling that promote cell adhesion and proliferation to occur.

Many experiments also had different surface modifications, with the goal being cellular adherence. Some research suggests that plasma treatments are sufficient in creating a microenvironment suitable for cellular adherence. Many commercially available tissue culture flasks are solely plasma treated, and at the macroscale, these flasks worked well for the adherent culture of NIH 3T3 fibroblasts. However, plasma treatment alone was insufficient in the experiments presented above. From there, all the devices were still plasma treated, but starting with Experiment 7 they were also coated in a 0.01% Poly-L-

Lysine solution. The specific coating procedures varied between experiments with the goal of finding the optimal coating protocol that was also time efficient.

Looking at the figures presented above, the results are largely inconclusive due to small samples sizes and limited experiment duplicates. Multiple one-way analysis of variance (ANOVA) were ran to examine variations in seeding density as a function of distance from the inlet, results of which are shown in **Figures 4.6** and **Figure 4.7**. While a uniform loading distribution is desired, a non-uniform loading distribution may not be the biggest concern for this project. As long as all wells had sufficient seeding for cell-to-cell signaling and adequate microenvironment control, the cells should be able to proliferate and adhere. Based on the material presented, no real distinct pattern is present in the seeding variation. While some statistical differences were observed, it is not believed to be relevant, again due to small sample size and large variation between protocols from experiment to experiment. Furthermore, when obtaining the cell solution for loading the device, flasks were used from varying confluences (~80-100%) which could account for the variation in seeding densities.

Multiple ANOVAs and Tukey's test were also ran looking at the average cell count in the device over time. One of two scenarios was expected: 1) an increase in cell count over time as the cells proliferated, or 2) a decrease in cell count due to cell death after nutrient depletion within the device created a microenvironment unsuitable for proliferation. However, the data collected reveals that the average counts remained largely consistent, even over multiple hours, as shown in **Figure 4.3-4.5** above. Some variations were observed due to perfusion attempts, which washed out many of the cells due to lack of adherence. While statistical differences were observed between different experiments, it

was not observed between time points within a single device. The variation between experiments is likely due to the variation in confluency of the flask used for each specific experiment and due to variation in procedural protocol, not due to proliferation as intended. Variation between experiments was expected because most experiments had a different experimental design, making comparison between experiments more difficult.

Smooth line graphs were also generated to look at each specific experiment's averages as a function of distance from the inlet and as a function of time. The goal was to look for any trends within the data for each specific protocol in order to identify the 'ideal' protocol for achieving adherent cell culture within the device. While the protocol presented in Experiment 12 appeared sufficient to achieve adherent cell culture, based on **Figure 4.14,** within the device, work still needs to be done to further optimize the procedure and to better recreate the ideal cellular microenvironment within the device. This includes better regulation of seeding density, CO_2 concentration, and nutrients via media perfusion.

The high surface-area-to-volume ratio of the device presented here posed unique difficulties for achieving adherent cell culture within the device. It is suspected that most nutrients were depleted from the device within three- and one-half hours. However, the cells were unable to attach sufficiently during that period, making it impossible to perfuse fresh media. While some experiments lasted longer than three- and one-half hours, it is highly unlikely that the cells had sufficient nutrients to adhere or proliferate.

6. CONCLUSION

The development of lab on a chip, micro total analysis systems, organ on a chip, and other similar technology has the potential to revolutionize the science and medical fields. Higher throughput experiments provide scientists with more data at a faster rate. A culture that takes months or years to develop and test at the macroscale could take days, maybe weeks, to develop and test at the microscale. While this helps with time and money, it also enables higher reproducibility and repeatability, which are paramount in clinical applications like drug development. Over 90% of drug animal models fail when translated to human applications [33]. This not only causes higher drug prices, but more importantly, it also means that only a very small number of drugs researched actually make it to market while billions of dollars and years were lost. Animal models currently are an important step in the pre-clinical development of drugs. However, microfluidics permits the development of systems that more accurately mimic the targeted *in-vitro* environment *in-vivo* and that can provide predictive human data. And data that can be obtained in days, maybe weeks, instead of months and years.

The future of science is trending toward microfluidics. From smaller sample sizes to higher throughput, microfluidics is a more cost effective and time efficient method compared to traditional macroscale experiments. The goal of this work was to develop the protocol for adherent cell culture within a microfluidic device. This included developing a protocol for successfully seeding the device, as well as developing the appropriate microenvironment that is sufficient for long-term, adherent cell culture. This work used the NIH 3T3 fibroblast cell line because it is robust and ultimately less

sensitive to variations within the microenvironment. However, the ultimate goal was to develop a protocol that could be adapted for any cell line and coculture.

The results presented in this report are inconclusive, however a lot of progress was made in developing a protocol for adherent cell culture within the microfluidic device.

7. FUTURE DIRECTIONS

Unfortunately, due to complications arising from Covid-19, the work presented here was terminated early. At the point of termination, multiple future experiments were planned to better achieve adherent cell culture within the device. Future experiments looked at better regulation of CO_2 levels and using centrifugation to remove trypsin from the cell solution prior to feeding, shown in the **Appendix** below. Here, I want to recommend a few potential experiments or modifications that will hopefully help future members of this project accomplish adherent cell culture.

7.1 Continuous Perfusion

One of the major limitations of my experiments was properly recreating the cellular microenvironment. Even with the robust, 'immortal' NIH 3T3 cell line, specific conditions need to be met in order for the cells to thrive. Based on my results and research, lack of nutrients greatly impacted the cellular environment. Many commercially available microfluidic devices for cell culture have depths ranging from $\sim 200 - 800 \mu m$ [23], which is roughly ten times larger than the device presented in this work. A common limitation of microfluidics devices is the higher surface-area-to-volume ratios compared to traditional tissue culture flasks and well plates [24]. In other words, there is less available volume for nutrients and waste storage in microculture.

There are two solution proposals that may combat this issue: using high glucose concentration media or increasing the serum in the media. Before constant perfusion is an option, the cells need to adhere to the surface: as long as the cells remain in suspension it is difficult to perfuse within the system. So, while neither of these proposals would be ideal for long term experimentation, they may be helpful during the initial stages of the

experiment. Using either of these proposals only during seeding and the first hour or two until the cells adhered and then using a pump, constant media perfusion could be implemented to supply sufficient nutrients and remove waste. The media used for these experiments was supplemented with 10% fetal bovine serum, but future experiments could look at using 15-20% to ensure sufficient nutrients. High glucose concentration DMEM is also commercially available. In that case, the device could be flushed with high glucose DMEM after the PLL incubation. When collecting the cells from macroscale culture, the trypsin could be neutralized using the high glucose DMEM, so that more glucose molecules per cell are present during the initially seeding. Improper neutralization of trypsin likely contributed to the inability of the cells to adhere. Moving forward it may be ideal to consider centrifuging the cell solution in a micro-centrifuge tube, which will form a pellet of cells in the bottom of the centrifuge tube and the media containing trypsin can be aspirated. Then the cells can be resuspended in fresh media before being seeded into the device. Furthermore, it is important to more closely regulate the pH and CO_2 concentrations within the device. Without proper CO_2 the pH in the system will not be suitable for cell proliferation and adherent culture. Proper CO_2 levels can be achieved by using an incubator during culture or developing a CO_2 feeder layer within the microfluidic network.

Another important consideration is the Effective Culture Time (ECT) and the Critical Perfusion Rate (CPR) [17]. For a $200\mu m$ channel, the ECT is between 8-12 hours. Based on a simple linear interpolation, the ECT is between 2.8-4.2hours for a $70\mu m$ channel. Ideally, then, the media within the device is replaced roughly every three hours, to ensure sufficient nutrient levels. Whether the media is perfused through the cell channel network

or through the nutrient generator will slightly alter the critical perfusion rate. Using the cell channel network, calculations propose a flow rate of $0.05 - 0.1\frac{\mu L}{hr}$. Using the gradient generator, a flow rate of approximately $1\frac{\mu L}{hr}$ should be sufficient. Perfusion through the gradient generator is the ideal option, so I propose a flow rate of $1\frac{\mu L}{hr}$ should be sufficient for long term culture within the device.

7.2 Bubbles

Bubble formation within a microfluidic device is incredibly problematic: often once a bubble is formed within the system it is virtually impossible to remove it. Added complications arise in microfluidic devices designed for cell culture because gases are a vital part in recreating the ideal microenvironment for cell adherence and proliferation. Media is a gaseous liquid, so bubbles can form even when all appropriate precautions are taken. One method for preventing bubbles from being introduced into the device is by adding a microscale bubble trap to the device [25]. A bubble trap could be added to future renditions of the device during the fabrication process. The trap could be placed where media and other gaseous liquids are introduced to the device.

7.3 Creating a Sufficient Microenvironment

Many factors are involved in creating the appropriate environment for cell culture. While a lot of these phenomena and factors are well understood at the macroscale level, they do not always easily translate to the microscale. This work looked at developing protocol for the use of a microfluidic device without traditional tissue culture equipment, specifically an incubator. An incubator helps regulate temperature and carbon-dioxide levels which are vital in creating a suitable microenvironment for cell culture adherence and

proliferation. Without using an incubator, regulating these conditions is more complicated. Aside from using an incubator, it may be possible to develop CO_2 a feeder layer within the device to regulate and maintain gas exchange within the device. In this scenario, 5-10% CO_2 could be constantly perfused into the system directly. It is also important to regulate the thickness of the PDMS to ensure optimal gas exchange can occur.

Another potential solution for having sufficient nutrients delivered to the cells continuously is to explore porous membranes/polymers that allow for diffusion of nutrients. We could create a dual layer microfluidic device with the porous membrane covered by the PDMS for sterility and structural integrity. This layer could help create an environment suitable for adherent cell culture during the periods where continuous perfusion is unideal. This way, nutrients could diffuse through the membrane without disrupting the cellular environment or creating a shear stress that washes the cells away before they have had sufficient time to adhere to the device.

WORKS CITED

[1] Jedrzejczak-Silicka, M. (2017). History of Cell Culture. In New Insights into Cell Culture Technology. InTech. https://doi.org/10.5772/66905

[2] Rous, P., & Jones, F. S. (1916). A METHOD FOR OBTAINING SUSPENSIONS OF LIVING CELLS FROM THE FIXED TISSUES, AND FOR THE PLATING OUT OF INDIVIDUAL CELLS. The Journal of experimental medicine, 23(4), 549–555. https://doi.org/10.1084/jem.23.4.549

[3] Frantz, C., Stewart, K. M., & Weaver, V. M. (2010). The extracellular matrix at a glance. Journal of cell science, 123(Pt 24), 4195–4200. https://doi.org/10.1242/jcs.023820

[4] Todaro, G., & Green, H. (2005). From the Archive A cell line that is under control, 168(7), 988–989.

[5] Hayflick L. (2000). The illusion of cell immortality. British journal of cancer, 83(7), 841–846. https://doi.org/10.1054/bjoc.2000.1296

[6] Material: PDMS (polydimethylsiloxane). (n.d.). Retrieved from http://www.mit.edu/~6.777/matprops/pdms.htm

[7] van Meer, B. J., de Vries, H., Firth, K., van Weerd, J., Tertoolen, L., Karperien, H., Jonkheijm, P., Denning, C., IJzerman, A. P., & Mummery, C. L. (2017). Small molecule absorption by PDMS in the context of drug response bioassays. *Biochemical and biophysical research communications*, *482*(2), 323–328. https://doi.org/10.1016/j.bbrc.2016.11.062

[8] Whitesides, G. M., Ostuni, E., Takayama, S., Jiang, X., & Ingber, D. E. (2001). Soft lithography in biology and biochemistry. *Annual review of biomedical engineering*, *3*, 335–373. https://doi.org/10.1146/annurev.bioeng.3.1.335

[9] Acord, K. (2020, October 21). Electrochemical Impedance Spectroscopy. Retrieved November 20, 2020, from https://eng.libretexts.org/Bookshelves/Materials_Science/Supplemental_Modules_(Materials_Science)/Insulators/Electrochemical_Impedance_Spectroscopy

[10] Hassan, Aslinda & Sheng, Siah & Md Shah, Wahidah & Bahaman, Nazrulazhar. (2018). An Automated Irrigation System Using Arduino Microcontroller.

[11] Probstein, R. F. (1989). 6.4 The Electric Double Layer and Electrokinetic Phenomena. In Physicochemical hydrodynamics: An introduction (pp. 185-191). Boston: Butterwoths.

[12] Little CAE, Orloff ND, Hanemann IE, et al. Modeling electrical double-layer effects for microfluidic impedance spectroscopy from 100 kHz to 110 GHz. Lab on a Chip. 2017 Jul;17(15):2674-2681. DOI: 10.1039/c7lc00347a.

[13] Khalili, A. A., & Ahmad, M. R. (2015). A Review of Cell Adhesion Studies for Biomedical and Biological Applications. *International journal of molecular sciences*, *16*(8), 18149–18184. https://doi.org/10.3390/ijms160818149

[14] Jedrzejczak-Silicka, M. (2017). History of Cell Culture. In *New Insights into Cell Culture Technology*. InTech. https://doi.org/10.5772/66905

[15] Su X, Theberge AB, January CT, Beebe DJ. Effect of microculture on cell metabolism and biochemistry: do cells get stressed in microchannels? Analytical Chemistry. 2013 Feb;85(3):1562-1570. DOI: 10.1021/ac3027228.

[16] Young, E. W., & Beebe, D. J. (2010). Fundamentals of microfluidic cell culture in controlled microenvironments. *Chemical Society reviews*, *39*(3), 1036–1048. https://doi.org/10.1039/b909900j

[17] Young, E. W., & Beebe, D. J. (2010). Fundamentals of microfluidic cell culture in controlled microenvironments. *Chemical Society reviews*, *39*(3), 1036–1048. https://doi.org/10.1039/b909900j

[18] Baracca, A., Sgarbi, G., Solaini, G., & Lenaz, G. (2003). Rhodamine 123 as a probe of mitochondrial membrane potential: evaluation of proton flux through F(0) during ATP synthesis. *Biochimica et biophysica acta*, *1606*(1-3), 137–146. https://doi.org/10.1016/s0005-2728(03)00110-5

[19] Keenan, T. M., & Folch, A. (2008). Biomolecular gradients in cell culture systems. *Lab on a chip*, *8*(1), 34–57. https://doi.org/10.1039/b711887b

[20] Hawkins, B. (2020.). [V3 Comsol model of Gradient Generator].

[21] Swenson, V. A., Stacy, A. D., Gaylor, M. O., Ushijima, B., Philmus, B., Cozy, L. M., Videau, N. M., & Videau, P. (2018). Assessment and verification of commercially available pressure cookers for laboratory sterilization. *PloS one*, *13*(12), e0208769. https://doi.org/10.1371/journal.pone.0208769

[22] PromoKine. Rhodamine 123 Mitochondria Stain Instruction Manual. April 2019. https://www.promocell.com/app/uploads/product-information/manual/PK-CA707-70010.pdf

[23] Kae SATO, Miwa SATO, Mizuho YOKOYAMA, Mai HIRAI, Aya FURUTA, Influence of Culture Conditions on Cell Proliferation in a Microfluidic Channel, Analytical Sciences, 2019, Volume 35, Issue 1, Pages 49-56, Released January 10, 2019, [Advance publication] Released November 23, 2018, Online ISSN 1348-2246, Print ISSN 0910-6340, https://doi.org/10.2116/analsci.18SDP04, https://www.jstage.jst.go.jp/article/analsci/35/1/35_18SDP04/_article/-char/en

[24] Su X, Theberge AB, January CT, Beebe DJ. Effect of microculture on cell metabolism and biochemistry: do cells get stressed in microchannels? Analytical Chemistry. 2013 Feb;85(3):1562-1570. DOI: 10.1021/ac3027228.

[25] Sung JH, Shuler ML. Prevention of air bubble formation in a microfluidic perfusion cell culture system using a microscale bubble trap. Biomedical Microdevices. 2009 Aug;11(4):731-738. DOI: 10.1007/s10544-009-9286-8.

[26] Svendsen, J. C. W. E. (2015). Lab-on-a-Chip Devices and Micro-Total Analysis Systems. Lab-on-a-Chip Devices and Micro-Total Analysis Systems. https://doi.org/10.1007/978-3-319-08687-3

[27] Grimnes, S. (2015). Chapter 4. Passive Tissue Electrical Properties. In 1039000796 795335284 O. G. Martinsen (Ed.), Bioimpedance and Bioelectricity Basics (3rd ed., pp. 77-118). Academic Press. doi:https://doi.org/10.1016/B978-0-12-411470-8.00004-0.

[28] Lerman, M. J., Lembong, J., Muramoto, S., Gillen, G., & Fisher, J. P. (2018). The Evolution of Polystyrene as a Cell Culture Material. *Tissue engineering. Part B, Reviews*, *24*(5), 359–372. https://doi.org/10.1089/ten.TEB.2018.0056

[29] Toepke MW, Beebe DJ. PDMS absorption of small molecules and consequences in microfluidic applications. Lab on a Chip. 2006 Dec;6(12):1484-1486. DOI: 10.1039/b612140c.

[30] Rejmontová, P., Capáková, Z., Mikušová, N., Maráková, N., Kašpárková, V., Lehocký, M., & Humpolíček, P. (2016). Adhesion, Proliferation and Migration of NIH/3T3 Cells on Modified Polyaniline Surfaces. *International journal of molecular sciences*, *17*(9), 1439. https://doi.org/10.3390/ijms17091439

[31] Useful Numbers for Cell Culture. (n.d.). Retrieved November 13, 2020, from https://www.thermofisher.com/us/en/home/references/gibco-cell-culture-basics/cell-culture-protocols/cell-culture-useful-numbers.html

[32] Dellaquila, A. (n.d.). The history of microfluidics. Retrieved November 13, 2020, from https://www.elveflow.com/microfluidic-reviews/general-microfluidics/history-of-microfluidics/

[33] Akhtar A. (2015). The flaws and human harms of animal experimentation. *Cambridge quarterly of healthcare ethics : CQ : the international journal of healthcare ethics committees*, *24*(4), 407–419. https://doi.org/10.1017/S0963180115000079

[34] Fulda, Simone & Gorman, Adrienne & Hori, Osamu & Samali, Afshin. (2010). Cellular Stress Responses: Cell Survival and Cell Death. International journal of cell biology. 2010. 214074. 10.1155/2010/214074.

[35] Sanderson, M. J., Smith, I., Parker, I., & Bootman, M. D. (2014). Fluorescence microscopy. Cold Spring Harbor protocols, 2014(10), pdb.top071795. https://doi.org/10.1101/pdb.top071795

APPENDIX

A. Design of Experiments

Experiment	Device	Sterilization		Temperature		Surface Treatments			Seeding Technique			Media Perfusion	CO_2	Responses
	v2	Ethanol/PA	Autoclave	RT	PT	Air Plasma	PLL	Laminin	Syringe Pump	Vaccum Suction	Centrifuge	None		
1	v2	+	-	+	-	+	-	-	+	-	-	+	-	No adherent culture
2	v2	+	-	+	-	+	-	-	+	-	-	+	-	No adherent culture
3	v2	+	-	+	-	+	-	-	+	-	-	+	-	No adherent culture
4	v2	+	-	+	-	+	-	-	+	-	-	+	-	No adherent culture
5	v2	+	-	+	-	+	-	-	+	-	-	+	-	No adherent culture
6	v2	+	-	-	+	+	-	-	+	-	-	+	-	No adherent culture
7	v2	+	+	-	+	+	-	-	+	-	-	+	-	No adherent culture
8	v2	+	+	-	+	+	-	-	+	-	-	+	-	No adherent culture
9	v2	+	+	-	+	+	+	-	+	-	-	-	-	No adherent culture
10	v2	+	+	-	+	+	+	-	+	-	-	-	-	No adherent culture
11	v2	+	+	-	+	+	+	-	-	+	-	-	-	No adherent culture
12	v2	+	+	-	+	+	+	-	-	+	-	+	-	Possible adherent culture
13	v2	+	+	-	+	+	+	-	-	+	-	+	+	No adherent culture
14	v2	+	+	-	+	+	+	-	-	+	-	+	+	No adherent culture
15*	v3	+	+	-	+	+	+	-	-	+	+	-	+	Terminated due to COVID-19
16*	v3	+	+	-	+	+	+	+	-	+	+	-	+	Terminated due to COVID-19
17*	v3	+	+	-	+	+	+	+	-	+	+	-	+	Terminated due to COVID-19
18*	v3	+	+	-	+	+	+	+	-	+	+	-	+	Terminated due to COVID-19

**Future Experiments unable to be performed due to early termination due to complications arising form COVID-19*